8.0 TETHERED OZONESONDE AND SURFACE OZONE MEASUREMENTS IN THE UINTA BASIN, WINTER 2013

Russ Schnell[1], Bryan Johnson[1,] Patrick Cullis[2], Chance Sterling[4], Emrys Hall[2], Rob Albee[3], Allen Jordan[2], Jim Wendell[1], Samuel Oltmans[2], Gabrielle Petron[2] and Colm Sweeney[2]

1. NOAA Earth System Research Laboratory, 325 Broadway, Boulder, CO
2. CIRES - University of Colorado, Boulder, CO 80305
3. Science and Technology Corporation, http://www.stcnet.com.
4. University of Colorado, Boulder, CO

8.1 Introduction

The four main goals of the NOAA ozone group involvement in the Uintah 2013 study were to:

1. Document the vertical and temporal distribution of the wintertime ozone production process in high resolution.
2. Collect data on the spatial distribution of ozone in the basin.
3. Determine whether the Bonanza power plant emissions are contributing precursors for ground level ozone production during temperature inversion (elevated ozone) events.
4. Determine where the ozone precursors originate.

Ozone and temperature profiles from the surface to 250-500 meters above ground level were measured January 24 - February 17, 2013 by tethered ozonesondes operated at Ouray Wildlife Refuge and Fantasy Canyon by the NOAA/ESRL Global Monitoring Division (GMD), and at Horsepool by the Institute for Arctic and Alpine Research (INSTAAR) from the University of Colorado with ozonesondes supplied by NOAA (Map, Figure 8-6). During this period, 735 vertical profiles of ozone, temperature and water vapor were conducted. Ozonesondes were also used to measure surface ozone from a vehicle on drives within the basin. Two free-flying ozonesondes were released during high surface ozone events to provide profiles from the surface to 30,000 meters, putting the surface measurements into perspective and to check for stratospheric intrusions of elevated ozone into the Uinta Basin. In a separate component of the Uinta 2013 study, NOAA flew an instrumented aircraft in the basin. These results are reported separately.

The 2013 study was the second consecutive winter that tethered ozonesondes were used within the Uinta Basin as part of campaigns investigating wintertime high ozone events. The winter conditions in the previous year (2012) were much different than in 2013 with warmer temperatures, the lack of snow cover and the absence of strong temperature inversions in 2012. Ozone measured in 2012 was within normal background ranges from 40-60 ppbv measured at all sites in the basin. The crucial difference in the meteorology influencing ozone formation in 2013 was the presence of persistent snow in the basin (Figure 8-1) and strong emission trapping temperature inversions.

All times are in local Mountain Standard Time (MST, mst) and all altitudes and elevations in meters (m) above sea level (asl).

Figure 8-1. The presence of snow throughout the Uinta Basin in 2013 was a controlling factor in the production of ozone in 2013 as discussed in various sections of this report.

8.1.1 Ozonesonde Measurements in the Uinta Basin

Ozonesondes have been used at NOAA for more than 25 years for monitoring stratospheric and tropospheric ozone at long term sites and in numerous intensive campaigns. The ozonesondes are typically released on free-flying balloons that reach 30-35,000 m altitude in less than 2 hours. However, for the Uinta Basin campaign, the relatively fast rising balloon (~ 300 meters per minute rise rate) on a typical ozonesonde flight would travel too quickly through the shallow layer of interest near the surface. Therefore, a new custom built tether system, shown in Figures 8-2 and 8-3, was designed to carry an ozonesonde from ground level to a height of 350 meters and back down in 60 minutes or less. Based on the 2011 ozone study within the Uinta Basin (Martin et al., 2011), this height would extend above the top of localized wintertime temperature inversions. Making two profiles per hour at three sites tracked the vertical development of the basin-wide wintertime photochemical ozone production and provided high resolution data for the study of the fine detail of the ozone formation and distribution. Vertical profiles for both ozone and temperature will be very useful to evaluate mesoscale model results.

Figure 8-2. An automated, portable NOAA tethered ozonesonde system at the Fantasy Canyon site. The tethered ozonesonde system was set up and in operation within an hour of arriving on site. The complete system is battery operated and can be left alone to conduct profiles to a pre-set altitudes, then return to the surface before repeating the cycle. The system will run for ~4 hours before sonde batteries require changing. *Photo: Patrick Cullis, NOAA/CIRES, February 2013.*

Figure 8-3. A portable NOAA automated ozonesonde tether installation in operation in the late evening at the Ouray Wildlife Refuge site. This system was operated remotely from within the staff house that also served as an ozonesonde preparation and calibration center. ***Photo: Patrick Cullis, NOAA/CIRES, February 2013.***

In 2013, in addition to the tethered ozonesondes, continuous UV Photometric surface ozone analyzers (TEI) (Figure 8-4) were operated full time at the Ouray National Wildlife Refuge and the Blue Feather pipe yard. The TEI at Ouray provided a comparison for the ozonesonde measurements. In Figure 8-5 is a plot of the Ouray tethersonde and TEI monitor data showing excellent agreement. The comparisons were conducted at the start and end of each tether profile by holding the ozonesonde for ~2 min next to the TEI inlet that was 1 meter above the snow surface. The TEI measurements were ~3 % lower than the ozonesonde measurements, but this is considered excellent agreement for ozone being measured with very different techniques. The ozonesonde measurements operate based on a quantitative chemical reaction, and air flow through the sample chamber is calibrated for each ozonesonde prior to its initial launch.

Figure 8-4. TEI UV photometric surface ozone analyzer operated full time at the Ouray Wildlife Refuge during the 2012 and 2013 campaigns. An additional unit was operated at the Blue Feather pipe yard in 2013.

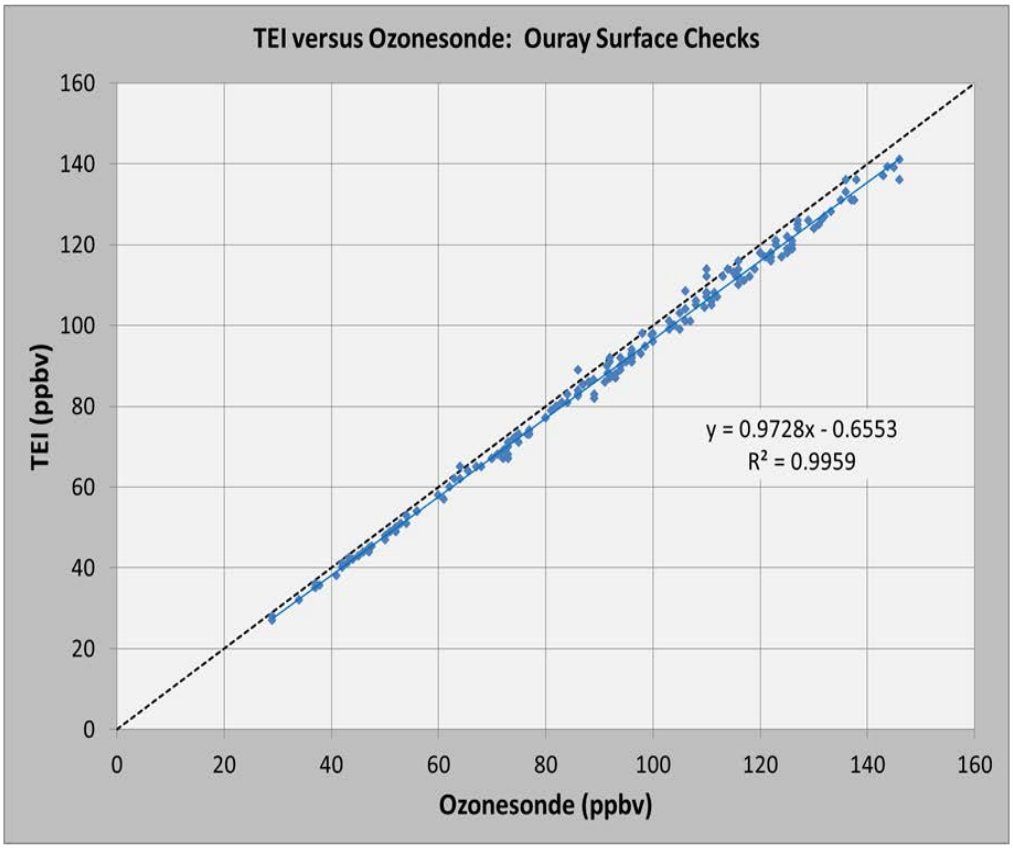

Figure 8-5. TEI versus ozonesonde measurements prior to each tethered ozonesonde profile ascent at the Ouray Wildlife Refuge site in 2013. The TEI reads about 3% lower than the ozonesondes. This is not considered a significant difference considering the range of ozone concentrations measured.

8.1.2 Ozonesonde Instruments

Ozonesondes are well-suited for vertical ambient and mobile measurements since they are stable under a wide range of temperatures and pressures. The measurement principle is based on the iodometric method, the fast reaction of ozone and iodide (I^-) in an aqueous 1% potassium iodide solution. The ozonesonde sensor described by Komhyr et al. (1969, 1995) uses a platinum electrode electrochemical cell. The sensor's output current is linearly proportional to the rate at which ozone is bubbled into the KI solution. Precision is better than ± (3–5)% with an accuracy of about ± (5–10)% up to 30 km altitude based on environmental chamber simulation tests reported by Smit et al. (2007), and from a field ozonesonde intercomparison campaign [Deshler et al., 2008]. Table 8-1 shows the specifications for the instruments used during the Uinta campaigns in 2012 and 2013.

The sensor is interfaced with an Imet radiosonde which measures and transmits ambient pressure, temperature, relative humidity and GPS altitude and location along with the ozone data.

The Uinta ozonesondes were conditioned and prepared according to NOAA standard operating procedures then compared to a NIST-standardized Thermo Environmental UV ozone monitor 49C operating continuously at the Ouray operations site. Final data was QA/QC'd using NOAA viewing and editing software.

Table 8-1. ECC (electrochemical concentration cell) Ozonesonde.

A. Ozonesonde Specifications

The ozonesonde sensor described by Komhyr et al. [1969, 1995] uses a platinum electrode electrochemical cell. The sensor's output current is linearly proportional to the rate at which ozone is bubbled into the KI solution. Ozone mixing ratio can then be computed from

Equation (1) $PO_3 = 4.30 \bullet (I - I_{BG}) \bullet Tp \bullet PF / P$

Where:
PO_3 = Ozone mixing ratio (parts per billion by volume)
I = Cell output current (~ 0-5.0 microamperes)
I_{BG} = Cell background current (typically 0-0.03 microamperes)
Tp = Temperature of sonde pump (K)
PF = Flow rate in seconds per 100 ml of air flow
Measured by a standard soap bubble flow meter with small correction (+2.5% to +3.5%) applied to account for evaporation of the soap bubble solution.
P = Ambient Air Pressure (hectopascals or millibars)

Accuracy Troposphere: ± 2 ppbv (parts per billion by volume) ± 3-5% of reading
Accuracy Stratosphere: ± (5–10%) up to 30 km altitude.
Precision: ± 3-5%

Data frequency: 1 hz

Calibration: No calibration is applied to the ozonesonde data. Ozonesondes are screened before use in the field by checking against the laboratory NIST-standardized Thermo Environmental UV ozone calibrator model 49C at zero, 40 ppbv and 100 ppbv. The ozonesonde must read within 2% of the calibrator before use in the field.

	Free flying release ozonesonde:	Tethered ozonesonde:
Altitude Range:	surface to 98,000 feet	surface to 1,000 feet
Balloon Rise Rate:	800 feet/ minute	35 feet/minute
Vertical Resolution:	160 feet	7 feet

B. InterMet Radiosonde Specifications

Temperature accuracy/precision: ± 0.2 C / 0.2 C

Humidity accuracy/precision: ± <3% / 2%

Pressure accuracy/precision: ±0.5hPa (millibars) / 0.5 hPa

GPS Altitude: +/- 5 meters (16 feet)

C. Thermo Scientific 49i Ozone Monitor Specifications

Principle: Dual path UV Absorption

Accuracy Troposphere: ± 1 ppbv (parts per billion by volume)

Precision: ± 3%

Range: 1-250 ppbv Calibration: NIST Traceable Data frequency: 1 minute averages

Table 8-2. Uinta Basin primary tethered ozonesonde site locations, number of profiles measured and maximum ozone mixing ratios measured during Jan and Feb, 2012 and 2013.

2012						
Location	Longitude (^{o}W)	Latitude (^{o}N)	Elevation (meters)	# of tether profiles/dates	[O_3]max (ppbv)	
Ouray	109.6446	40.1347	1430	42 Feb 6-27	54	
Horsepool	109.4674	40.1431	1569	62 Feb 7-26	59	
Jensen	109.3519	40.3687	1454	33 Feb 6-28	47	
Roosevelt	110.0082	40.2943	1587	8 Feb 16	51	
2013						
Locations	Longitude (^{o}W)	Latitude (^{o}N)	Elevation (meters)	# of tether profiles/dates	[O_3]max (ppbv)	
Ouray	109.6446	40.1347	1430	387 Jan 24 - Feb 7	167	
Horsepool	109.4674	40.1431	1569	216 Jan 24 - Feb 17	162	
Fantasy Canyon	109.3941	40.0582	1470	132 Jan 31 - Feb 7	152	

8.1.3 Tethered Ozonesonde (Tethersonde) Measurements

The ozonesonde tether system was developed by the NOAA Global Monitoring Division for the Uinta Basin field projects. The system is based upon a motorized deep sea fishing rod and reel with 50 pound line. The design includes communication software and data loggers to continuously monitor the radiosonde pressure allowing control of the ascent and descent rates. Temperature and dew point are radioed to the surface in real time as is GPS altitude and Latitude/Longitude coordinates of the instrument package. The system can operate unmanned during ascent and descent and can maintain a level altitude controlled from a laptop computer.

The tethered balloon sites are presented in Figure 8-6 with gas and oil wells shown in blue and red respectively. The sites are also listed in Table 8-2 along with the maximum ozone levels (mixing ratios – parts per billion (ppb) by volume) observed in 2012 and 2013 during the two wintertime campaigns. The absence of high concentrations of surface ozone in 2012 (Figure 8-7) is clearly observed in the ozone vertical profiles when compared to 2013 shown in Figure 8-8.

The NOAA ozone group has collected and processed a huge amount of data in this project. For instance, we have plotted ~1750 graphs and have over a million lines of discrete data files. For this report, we show the minimum number of graphs and analyses to present a cohesive story without overwhelming the reader. All of the 2013 data and graphs may be accessed at: ftp://ftp.cmdl.noaa.gov/ozwv/ozone/Uintah_2013_Tether_OzoneSondes/ .

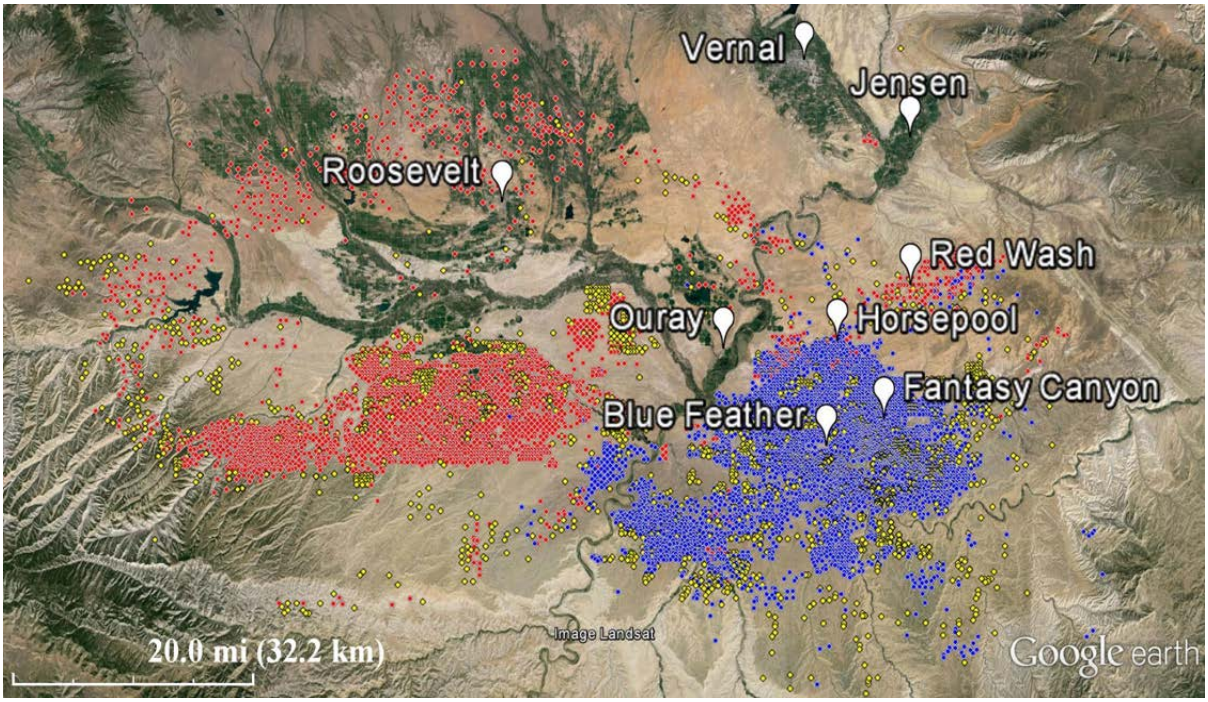

Figure 8-6. Map of the Uinta Basin with locations of the oil (red) and gas wells (blue) and the tethersonde sites in 2012 (Ouray, Horsepool, Roosevelt and Jensen) and 2013 (Ouray, Horsepool and Fantasy Canyon). Surface ozone monitors were operated at Blue Feather and Ouray in 2013. There is an EPA ozone monitor at Red Wash that the mobile ozone van passed regularly.

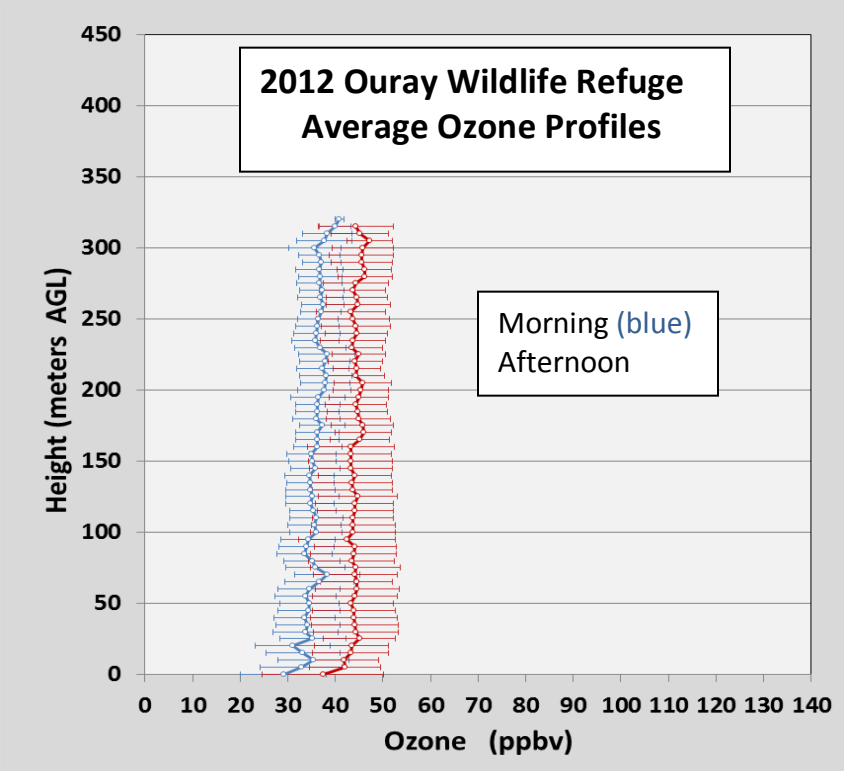

Figure 8-7. Summary plot of the 2012 average ozone mixing ratios and standard deviations measured at all sites during morning (between sunrise and local noon, in blue) and afternoon (noon to sunset, red). Note the absence of any large ozone production in events in 2012 compared to the range of the ozone measured in 2013 presented in Figure 8-8. The data in Figures 8-7 and 8-8 are plotted on the same scales binned at 5 m elevations.

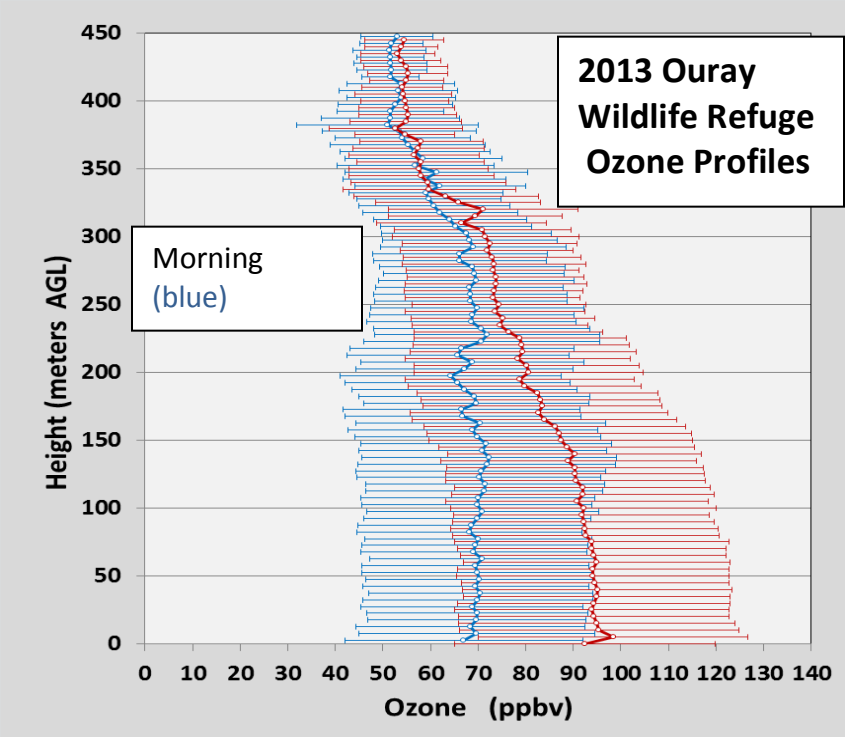

Figure 8-8. Summary plot of the 2013 average ozone mixing ratio and standard deviations measured at all sites during morning (between sunrise and local noon, in blue) and afternoon (noon to sunset, red). Note the large range of ozone concentrations in 2013 and the large photochemical production of ozone in the afternoons. The data in Figures 8-7 and 8-8 are plotted on the same scales.

8.2 Uinta Basin 2013 Surface Ozone Concentrations

8.2.1 Surface and Tethersonde Measurements at Three Sites

Surface ozone concentrations measured between January 15 and February 15, 2013 at Ouray Wildlife Refuge (NOAA), Red Wash (EPA) and Horsepool (NOAA) are presented in Figure 8-9. In this figure three successive wintertime high ozone production events may be observed. The diurnal ozone production cycle and the ozone build-up over time are in clear evidence. The rapid drops in ozone at the end of each cycle are caused by "cleanout" events that occur when fresh air or storms from outside the basin flush out the ozone and ozone precursors that are trapped below shallow, basin wide temperature inversions.

The successive colored arrows point to times that ozonesonde profiles are presented in Figures 8-10 - 8-15. In these figures we show that ozone and temperature profiles were remarkably similar at the three well-distributed sites that are at different elevations. This shows that the inversion layer is relatively constant in altitude across the basin and independent of the height of the surface topography. This constant altitude inversion layer is also observed in the aircraft and surface mobile measurements.

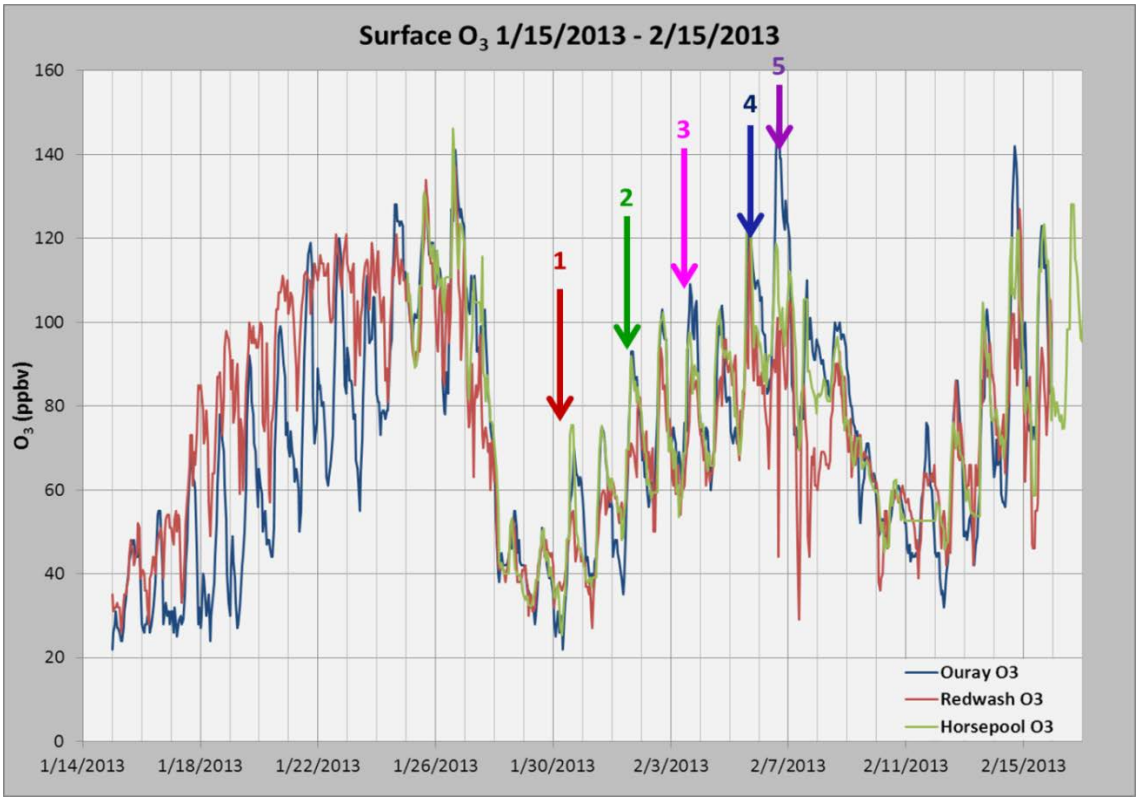

Figure 8-9. Surface hourly average ozone concentrations measured at three dispersed sites in the Uinta Basin showing the diurnal production of ozone, the build-up of total ozone during an event and the rapid cleanout of the basin that occurs when air from outside the basin enters and mixes down to the surface.

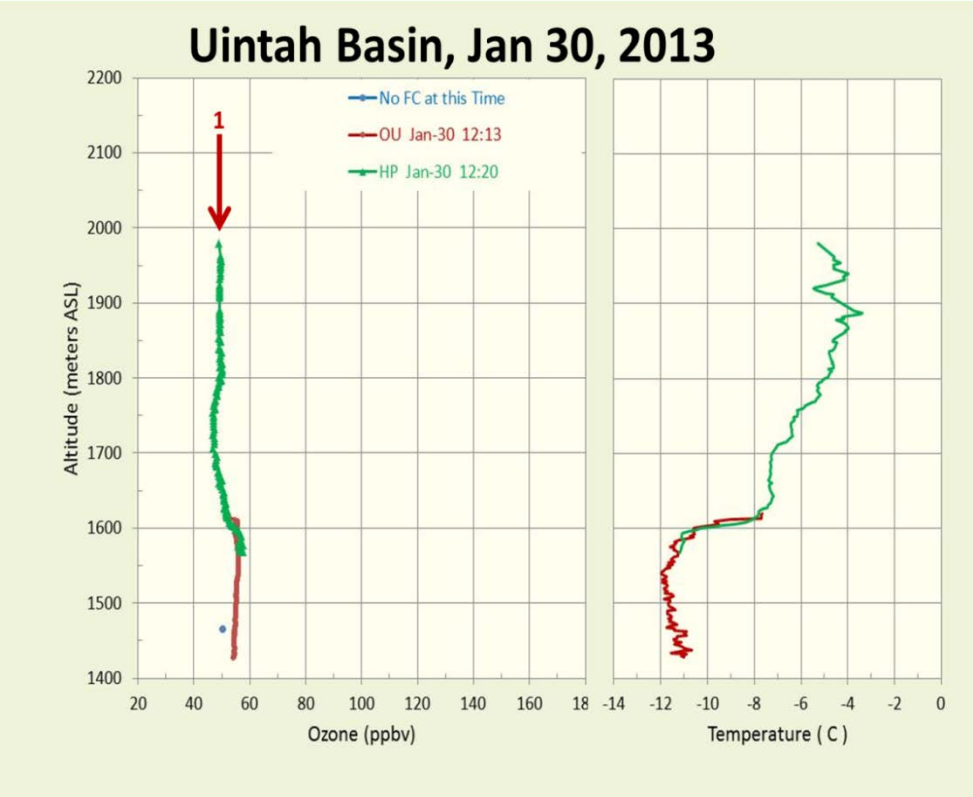

Figure 8-10. Ozone and temperature profiles from Ouray (OU) and Horsepool (HP) showing that ozone and temperature profiles were similar at these two site separated by 15.1 km in distance and 139 m in elevation. Note the cold surface temperatures and sharp temperature inversion at 1600 m, but no ozone difference across the inversion.

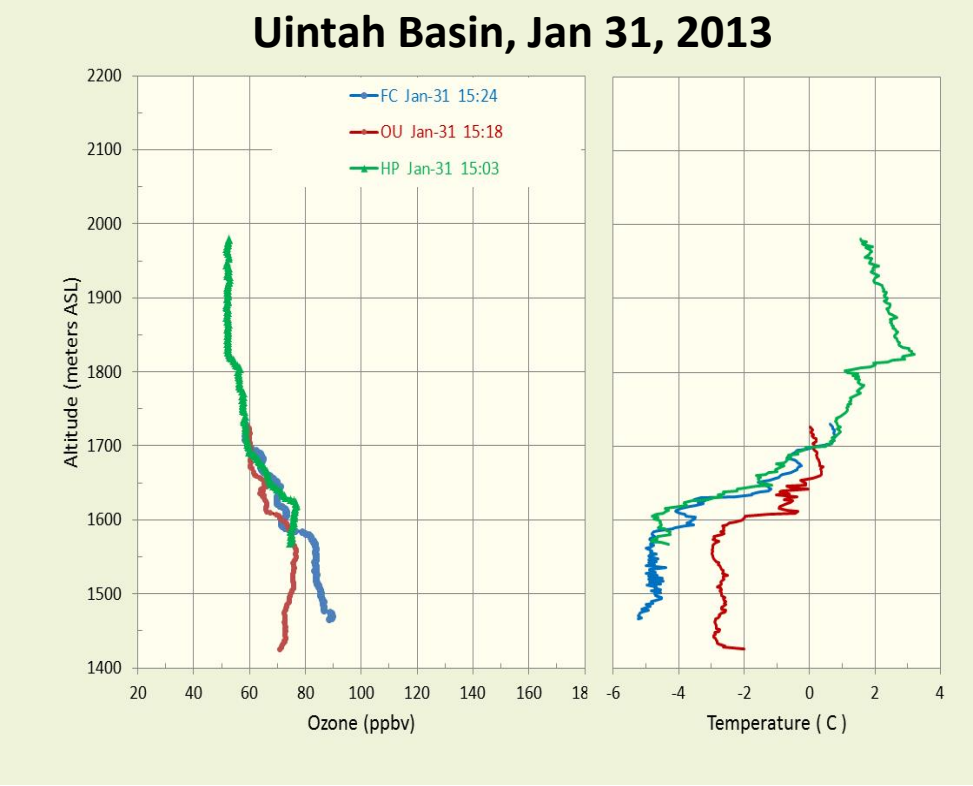

Figure 8-11. Ozone and temperature profiles from Ouray (OU), Fantasy Canyon (FC) and Horsepool (HP) showing that ozone began increasing on January 31.

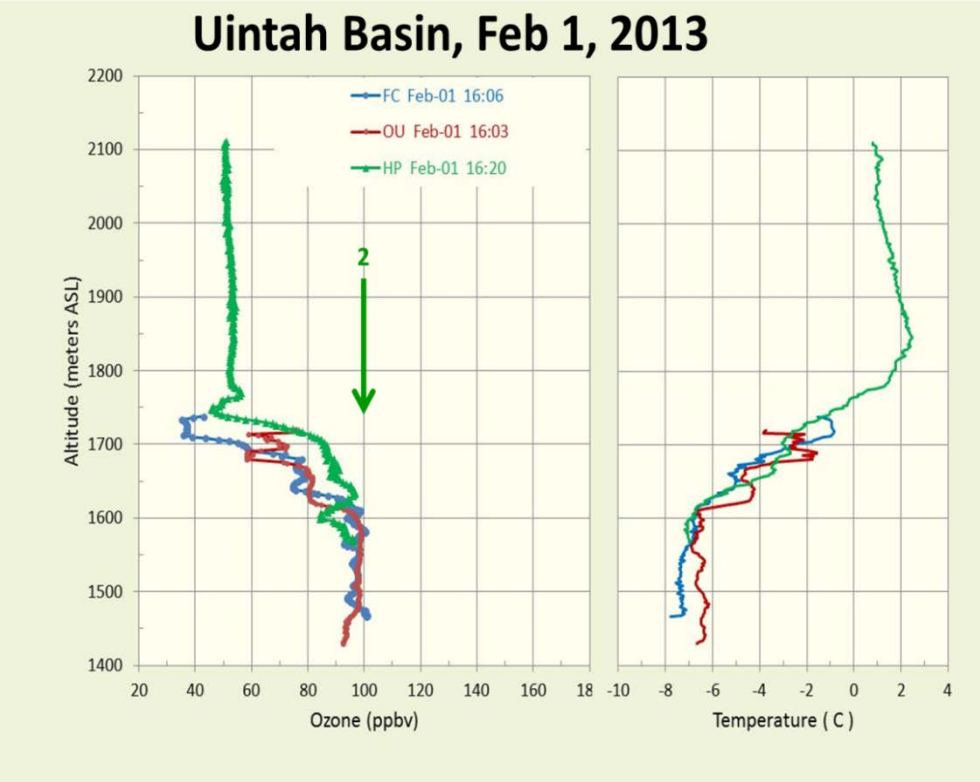

Figure 8-12. Ozone and temperature profiles from Ouray (OU), Fantasy Canyon (FC) and Horsepool (HP). Fantasy Canyon and Ouray are separated by 23 km in distance and 43 m in elevation with Ouray being lower. Note the build-up of ozone between the surface and 1700 m beneath the top of the temperature inversion layer.

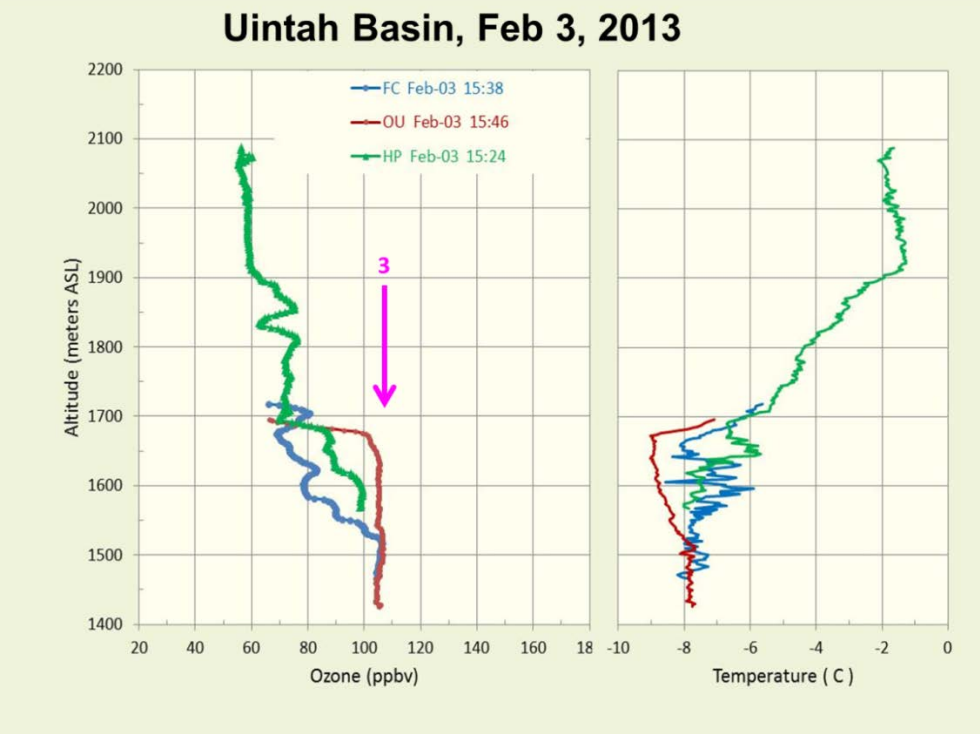

Figure 8-13. Ozone and temperature profiles from Ouray (OU), Fantasy Canyon (FC) and Horsepool (HP) Feb 3, 2013. The accumulation of ozone was somewhat different now at the three sites with Ouray exhibiting higher concentrations than Fantasy Canyon or Horsepool.

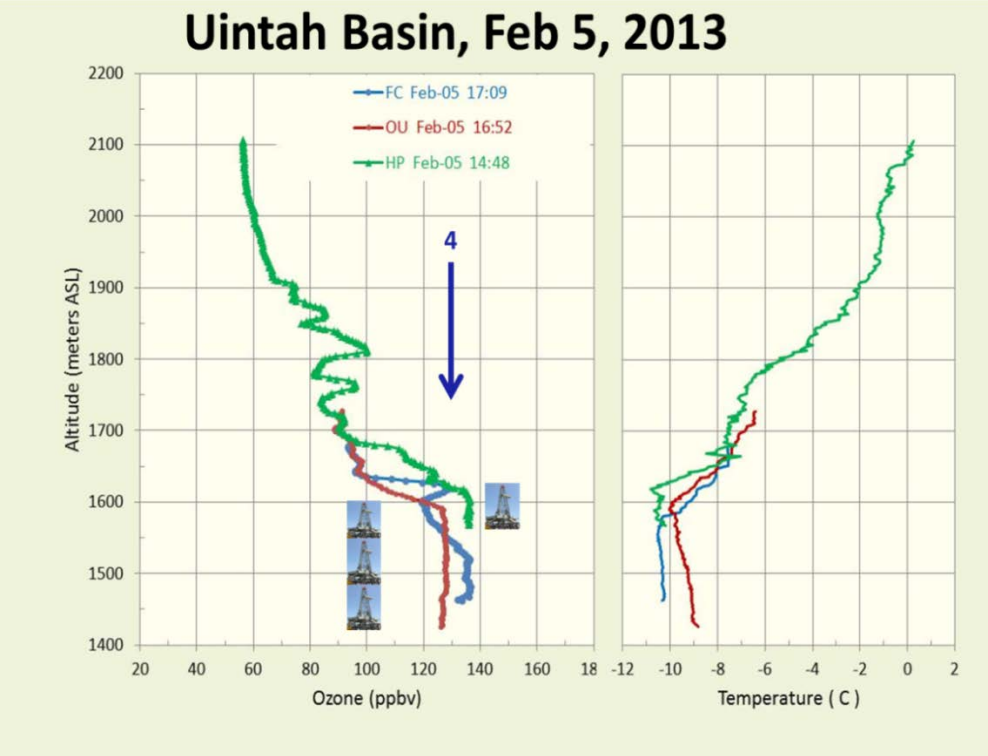

Figure 8-14. Ozone and temperature profiles from Ouray (OU), Fantasy Canyon (FC) and Horsepool (HP) showing the depth of the ozone layer relative to the height of a 150 foot tall drill rig. This emphasizes how shallow the ozone layer is, especially at Horsepool, which is at a higher elevation than the Ouray or Fantasy Canyon sites.

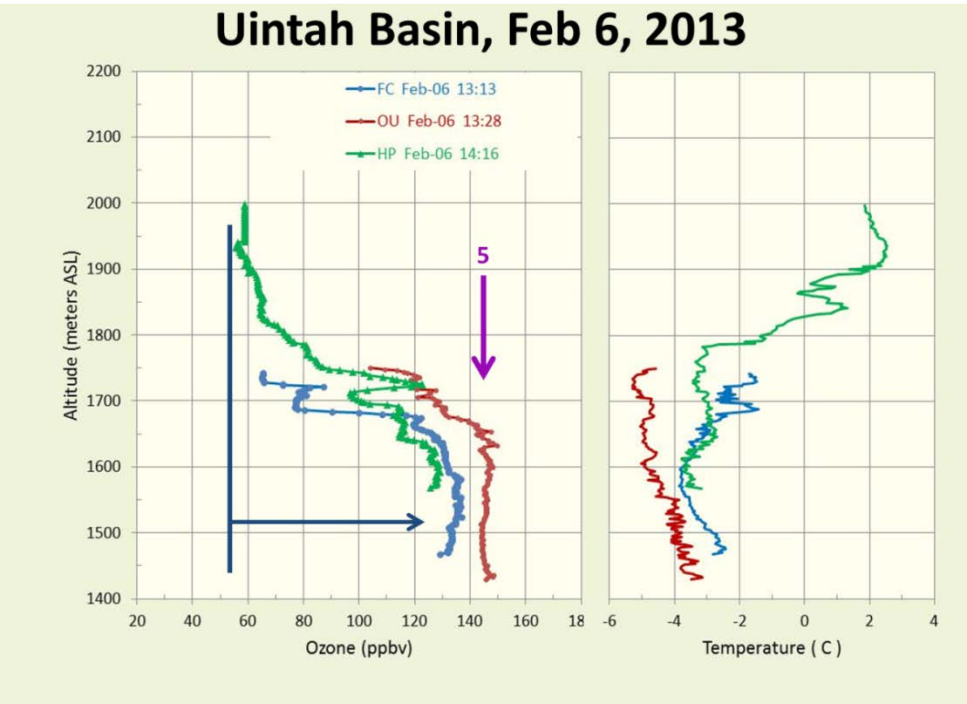

Figure 8-15. Ozone and temperature profiles from Ouray (OU), Fantasy Canyon (FC) and Horsepool (HP) near the peak in an ozone event. Note how the ozone production is confined to a shallow surface layer and is greater at Ouray which is at a lower elevation in the basin.

8.2.2 Diurnal Ozone Regression and Production during an Ozone Event

As is observed in Figure 8-9, photochemical ozone production is diurnal in nature, reaching a peak in the afternoon then falling off at night. During a major ozone event, between flushings of the basin air, ozone accumulates in a fairly steady rate of ~ 10 ppb/day on a day-to-day basis. In Figures 8-16 through Figures 8-28 are presented tethersonde profiles of ozone measured from the Ouray Wildlife Refuge January 27 – February 6, 2013. The presentation begins with the retreat of ozone concentrations on January 27 (Figure 8-16) from the flushing of the basin with air from the west. The cleanout continued through January 28 (Figure 8-17). On January 29 (Figure 8-18) there was no ozone production in the clean air at the Ouray site. The profiles presented are a small selection of those available in the archive.

On January 30 (Figure 8-19), ozone concentrations in the inversion surface layer at Ouray were less than 30 ppb near the surface with ozone production progressing steadily throughout the day, reaching 78 ppb by 18:03. A similar pattern was observed on January 31 (Figure 8-20). On February 1 (Figure 8-21), ozone production was substantially enhanced over the prior day, reaching just below 100 ppb in the 16:03 and 16:38 profiles. Ozone concentrations did not decrease to background levels overnight and on the morning of February 2 (Figure 8-22) and ozone increased to 105 ppb at Ouray in the 17:16 profile. A similar pattern was observed on February 3 (Figure 8-23) and February 4 (Figure 8-24), but the peak in ozone occurred later in the day at 18:39 on February 4. On February 5 (Figure 8-25), ozone was 80+ ppb by 10:01 and increased to 127 ppb by 16:23 and held there through the last profile at 18:41.

Ozone concentrations remained elevated throughout the night and were at 100+ ppb in the 10:10 profile on the morning of February 6 (Figure 8-26) rising to 165 ppb in the 13:50 profile. After the 13:50 profile, cleaner air began to move into the Uinta Basin at upper levels and by 17:31 ozone concentrations above 1550 m altitude had dropped 85-90 ppb into a 72-78 ppb range. This refreshing of the air from above and then partial recovery of the ozone is illustrated in Figure 8-27 for the same day where the ozone peak at 13:50 is seen to drop up to 16:43 and then partially recover as ozone rich air is sloshed back over Ouray, as illustrated in the 18:15 profile. The cleanout of the basin was not complete on February 6 and by the afternoon of February 7 (Figure 8-28) ozone production added an additional 20 ppb between 11:08 and 13:53. The last profile was taken at 15:11 showing a well-mixed 100 ppb from the surface to 1760 m.

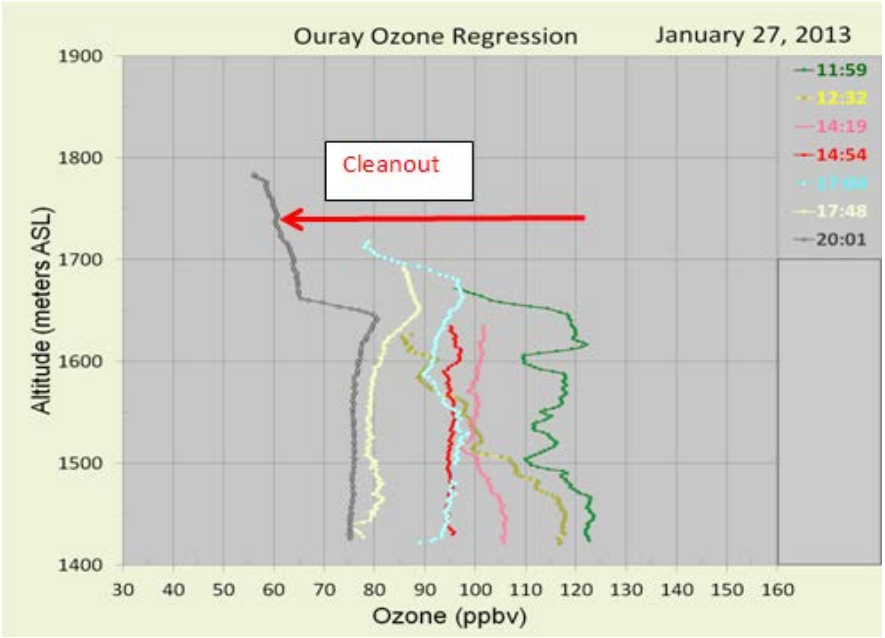

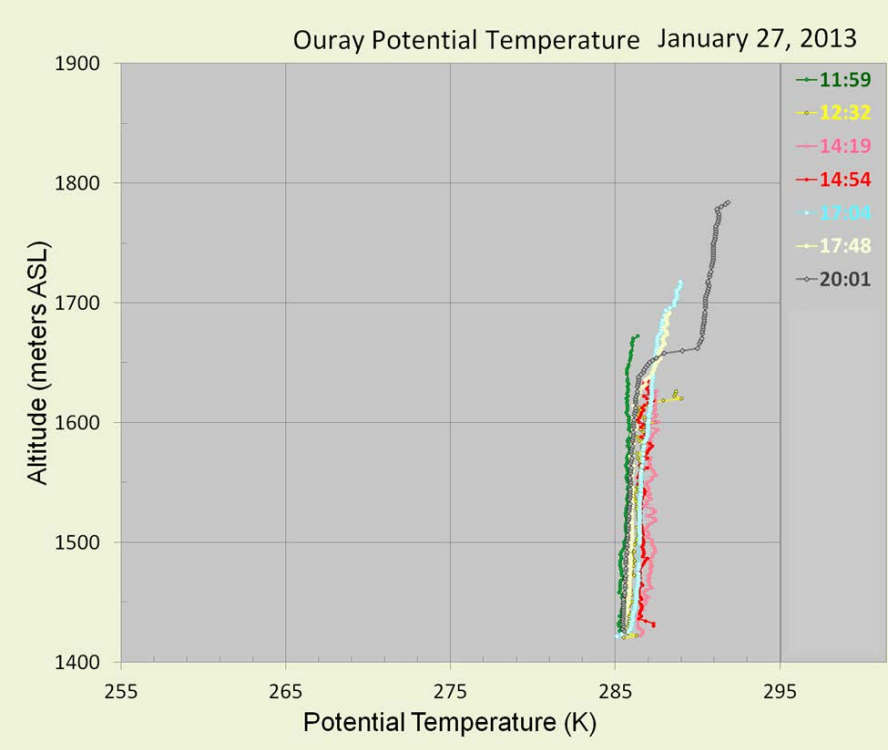

Figure 8-16. Ozone profiles from the Ouray Wildlife Refuge site (OU) showing that ozone in the 120 ppb range in the noon (11:59) profile decreased during the day to 75 ppb as cleaner air from the west flushed out the stagnant methane and ozone laden air of the previous stagnation event. (Lower) The corresponding potential temperature profiles were constant over this same period with the profile at 2001 showing that mixing of the lower level air was becoming capped in the evening at ~1650 m.

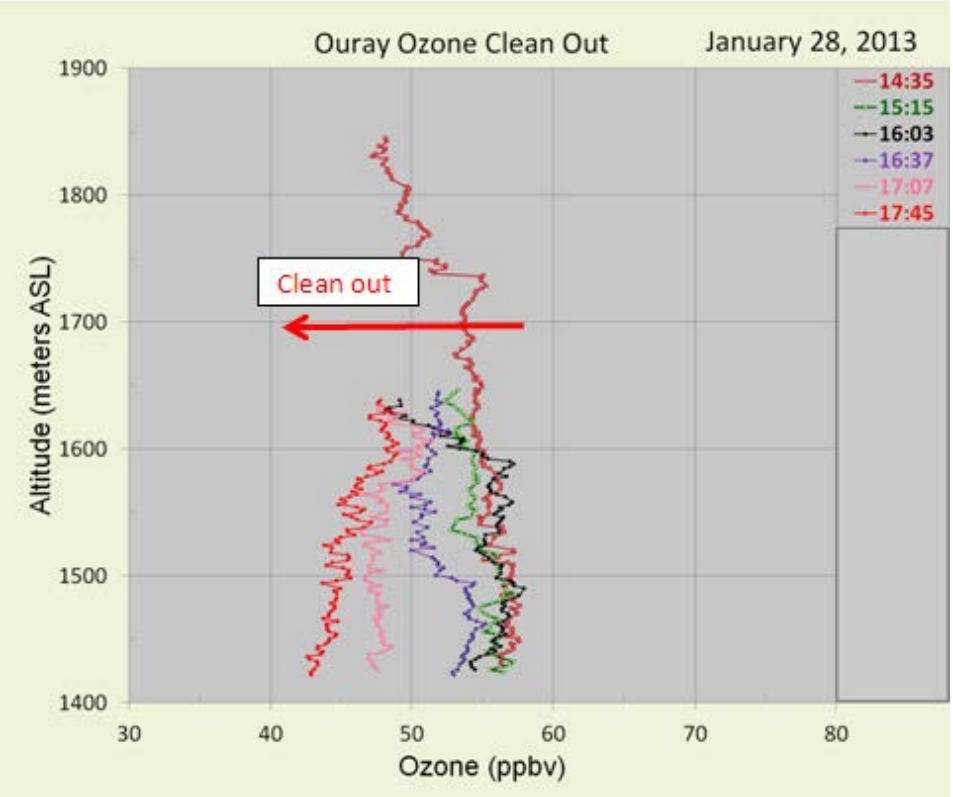

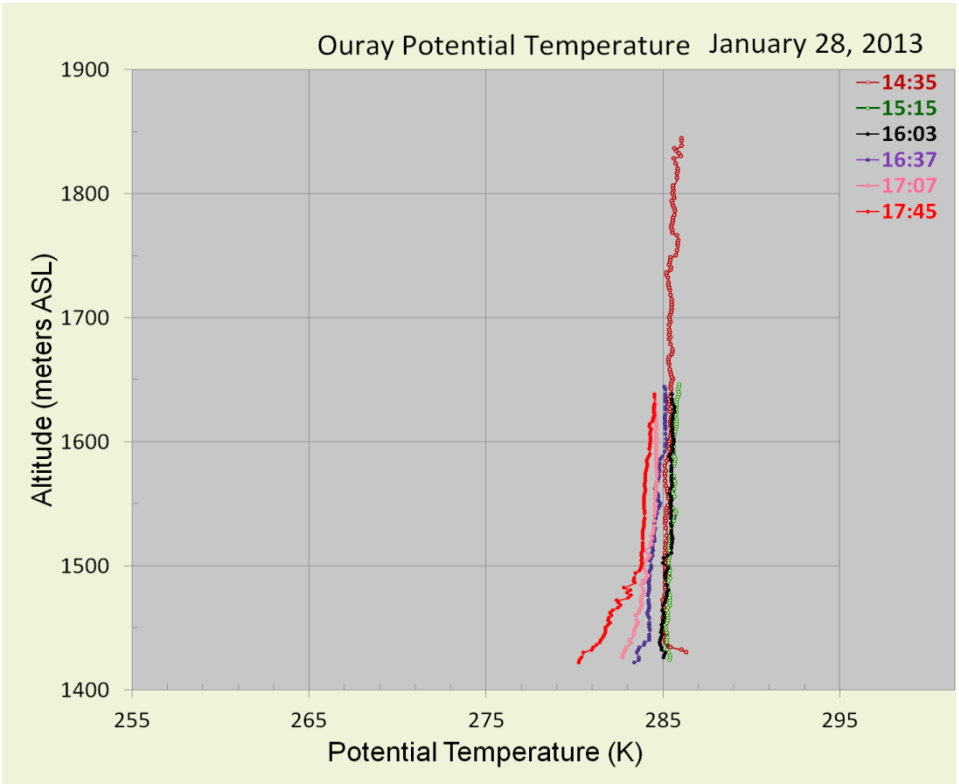

Figure 8-17. (Upper) Ozone profiles from the Ouray Wildlife Refuge site (OU) showing that as the flushing (cleanout) of the basin progressed, ozone decreased throughout January 28. (Lower) Corresponding potential temperature profiles showed that well-mixed air was entering the basin and that a weak temperature inversion was beginning to develop near the surface in the evening (17:45 profile).

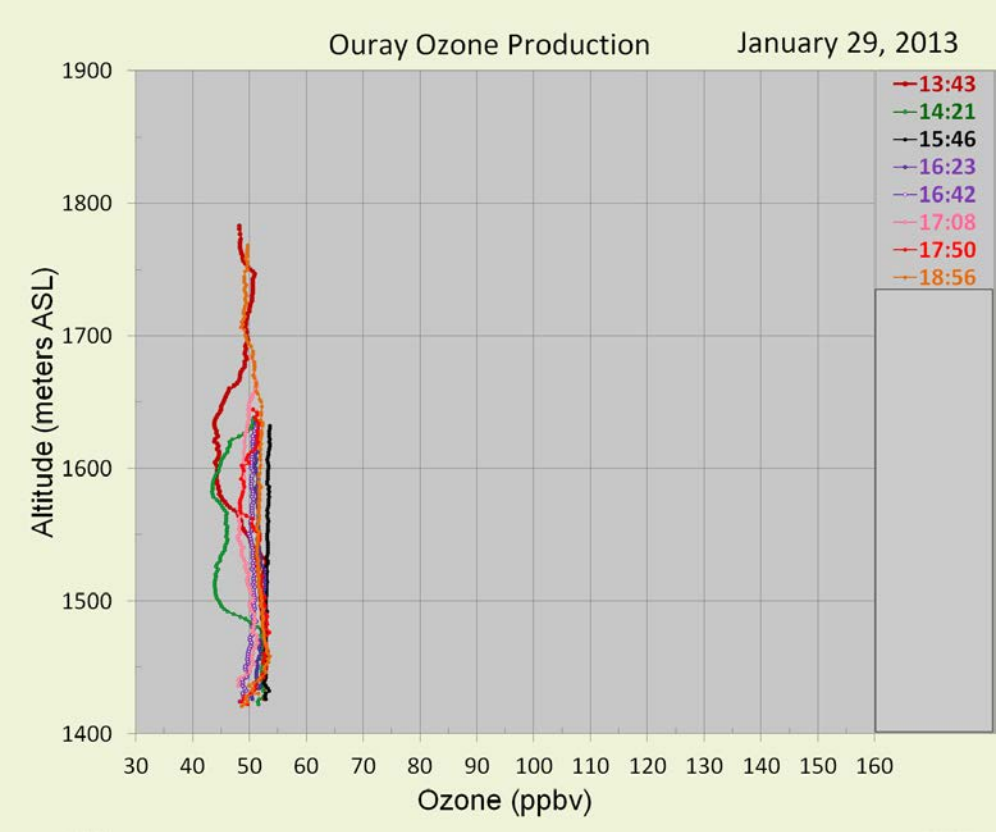

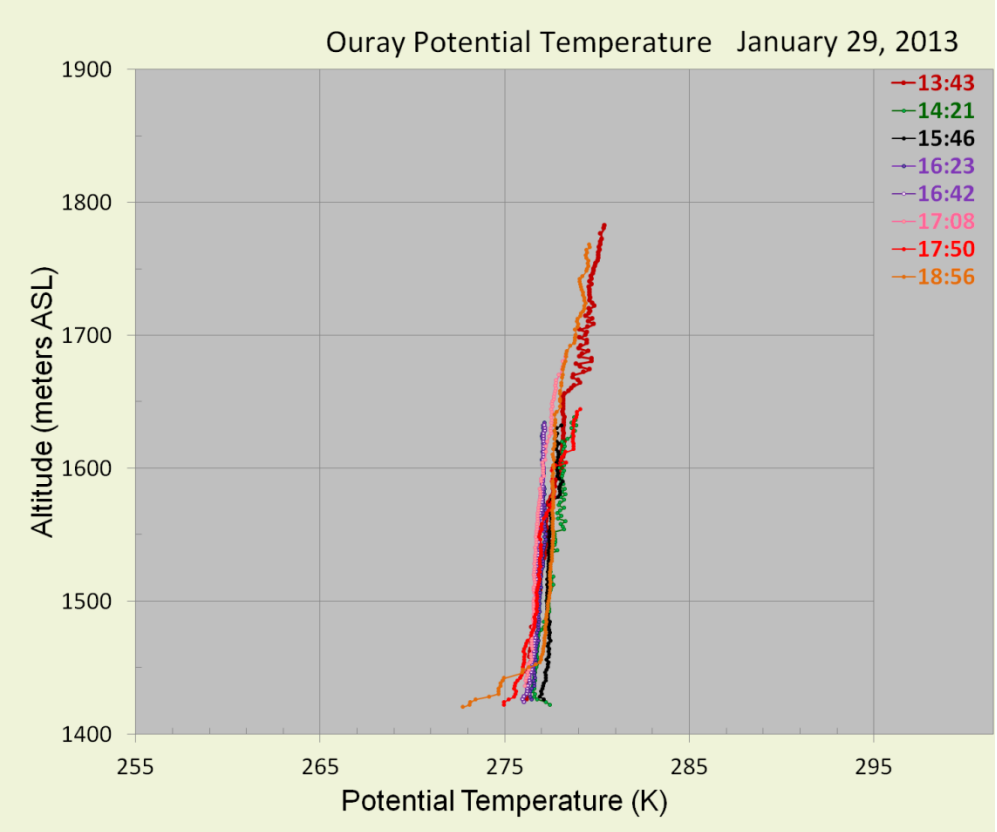

Figure 8-18. (Upper) By January 29 the basin was flushed out and there was no photochemical ozone production as all the profiles were at background levels throughout the day. (Lower) Potential temperatures show that the air mass was becoming slightly more stable with a shallow temperature inversion developing near the surface in the evening.

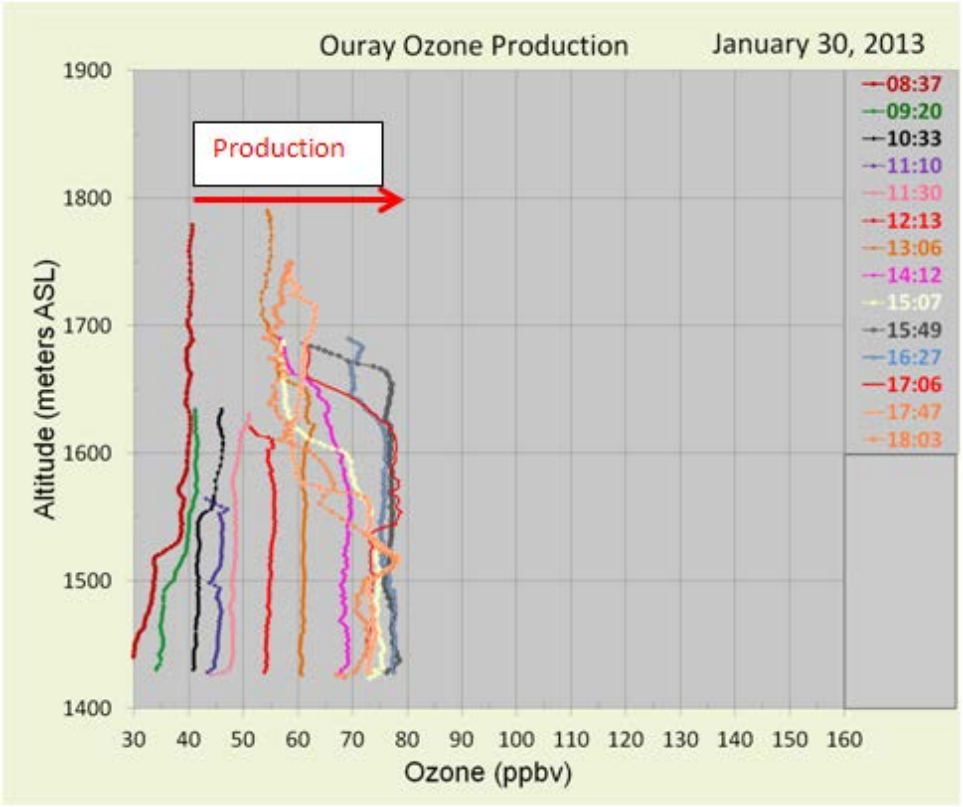

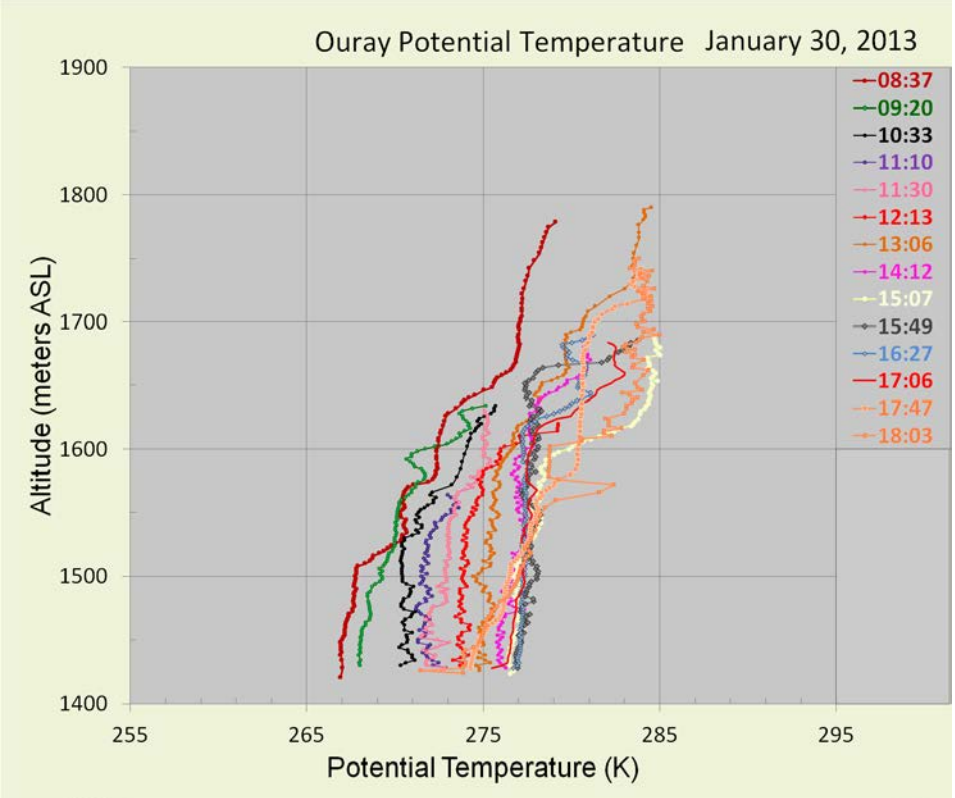

Figure 8-19. (Upper) By January 30 ozone precursor emissions were collecting in the basin and photochemical ozone production rose from a low of 30 ppb at sunrise to 78 ppb by 15:49. (Lower) Potential temperatures show that the atmosphere was becoming appreciably more stable with a strong inversion base developing at 1600 m.

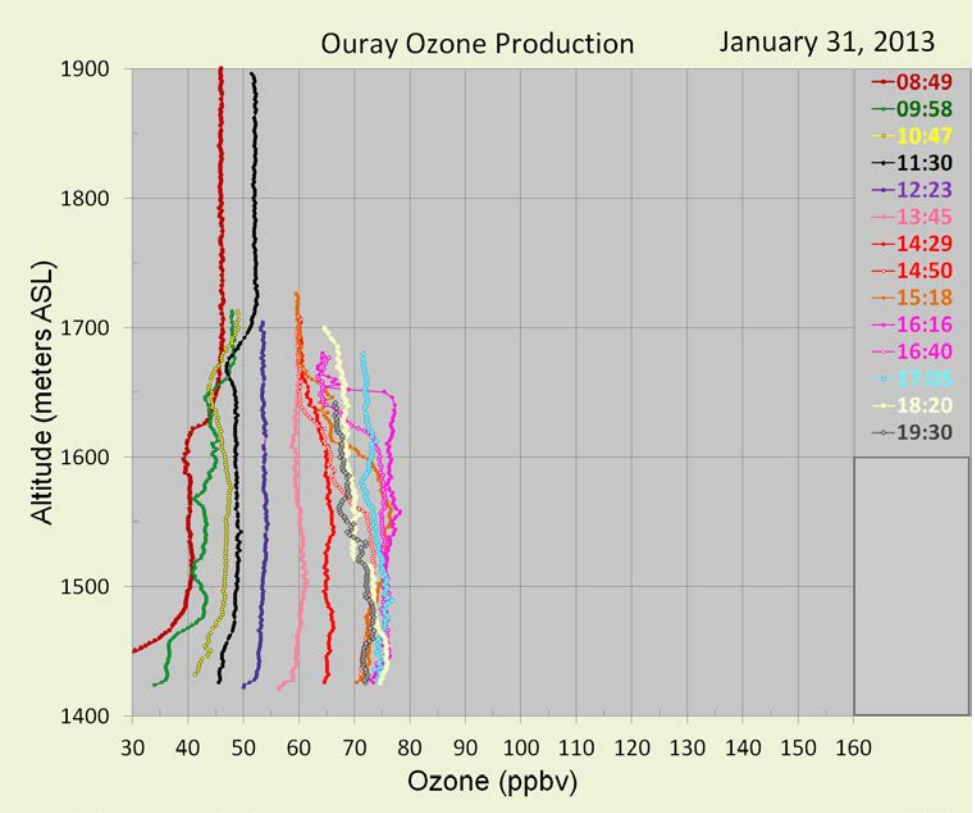

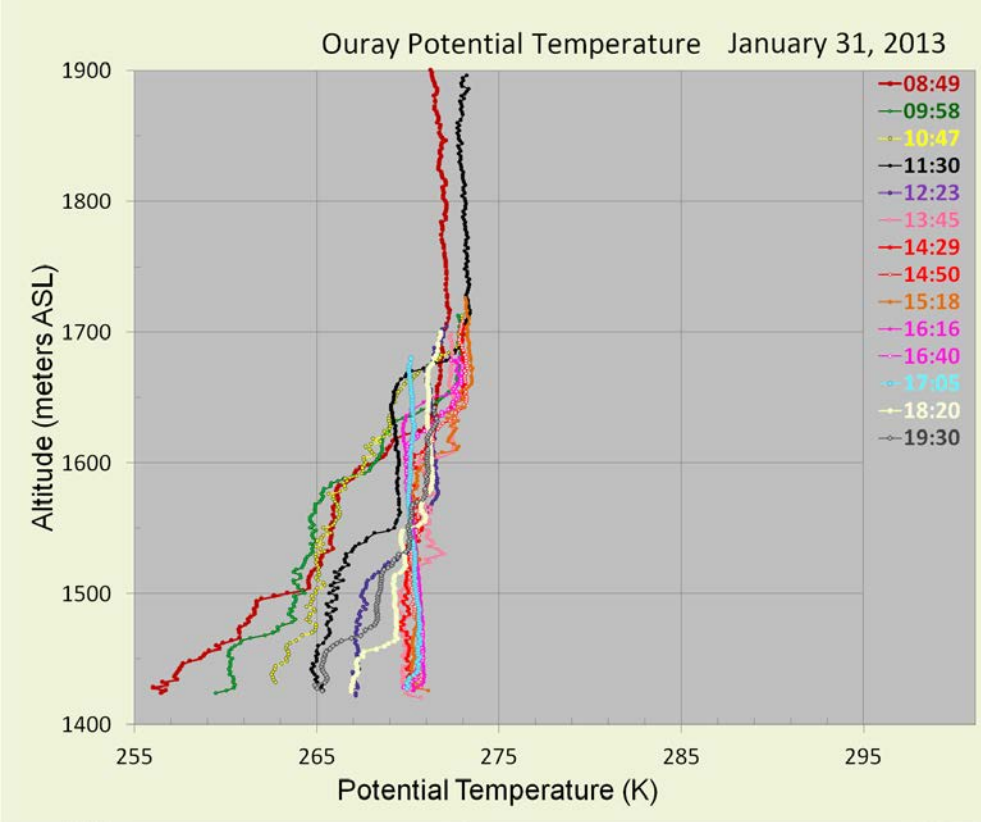

Figure 8-20. (Upper) Ozone production on January 31 was similar to January 30 with no large carryover of ozone from the previous day. (Lower) Potential temperatures decreased and the air remained stable beneath 1650 m.

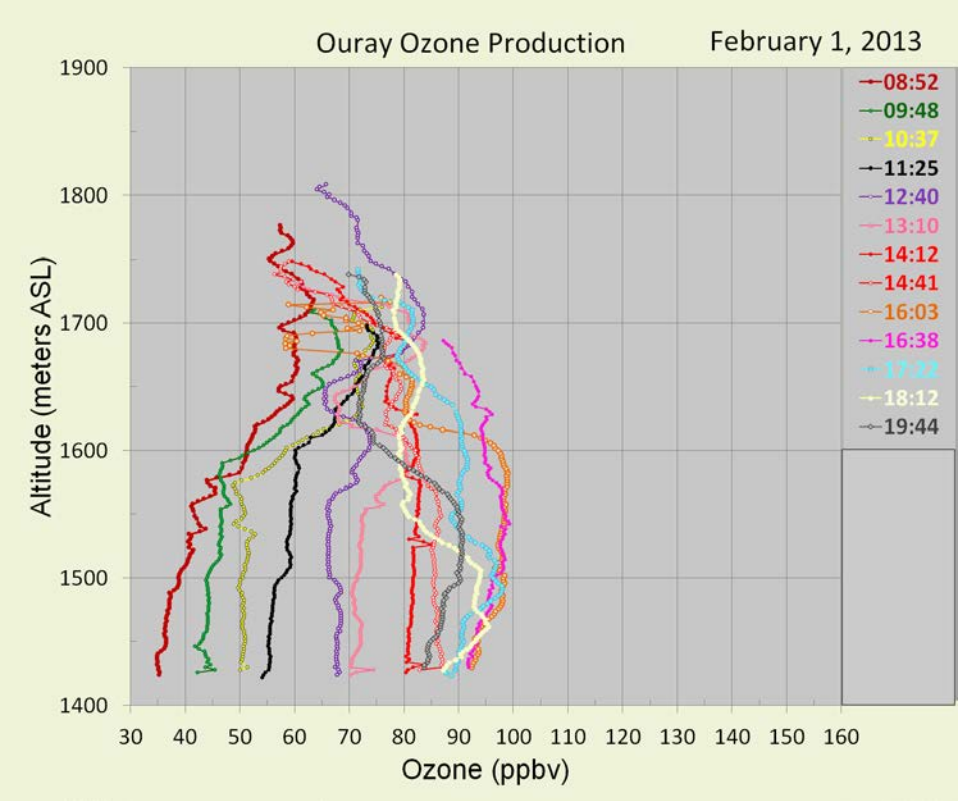

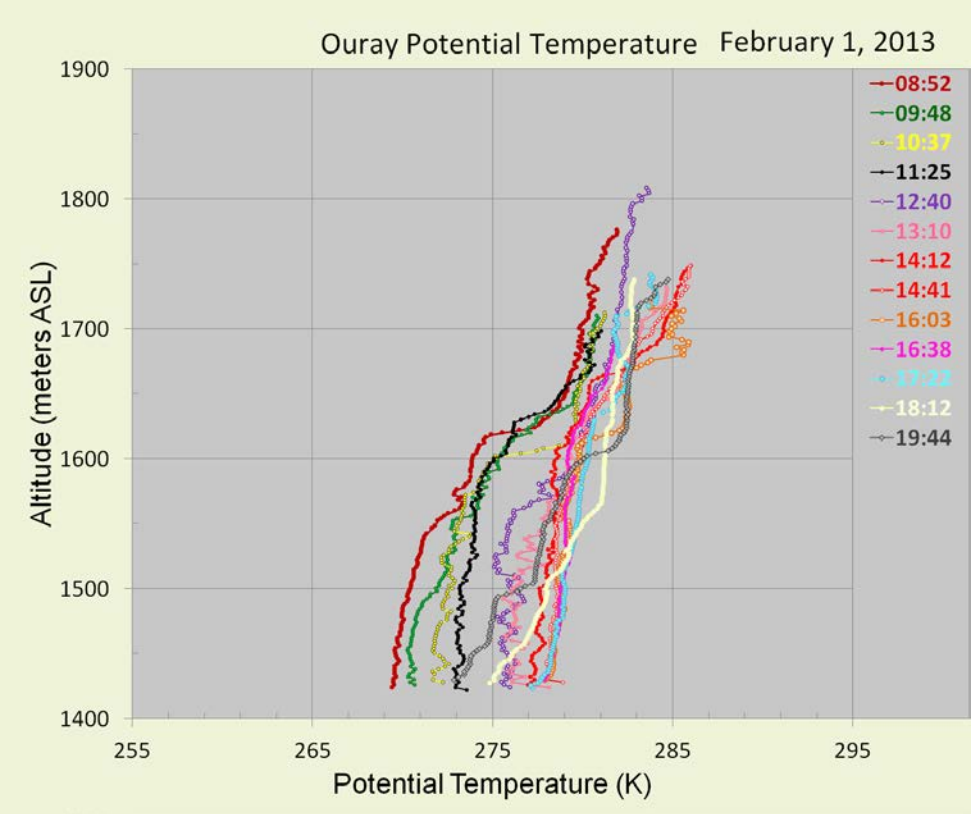

Figure 8-21. (Upper) On February 1 ozone production substantially increased over the previous day reaching 100 ppb in the 13:10 profile then decreasing to 60 ppb after sunset. (Lower) The potential temperature plots show that the atmosphere was very stable with the inversion top maintained at just above 1600 m.

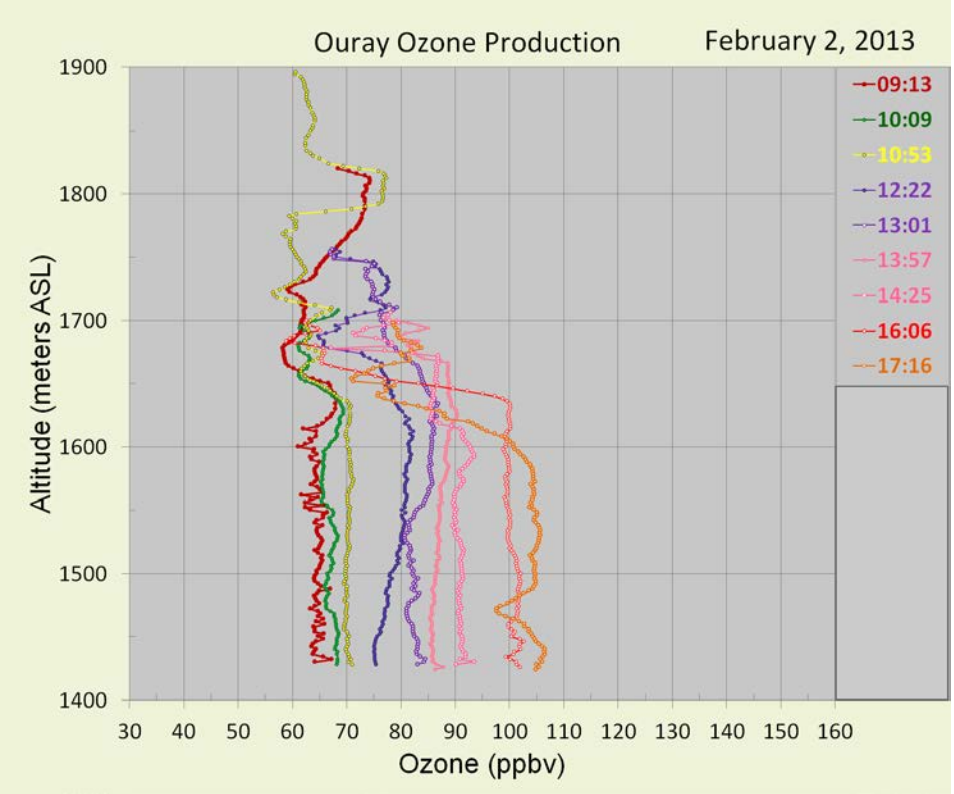

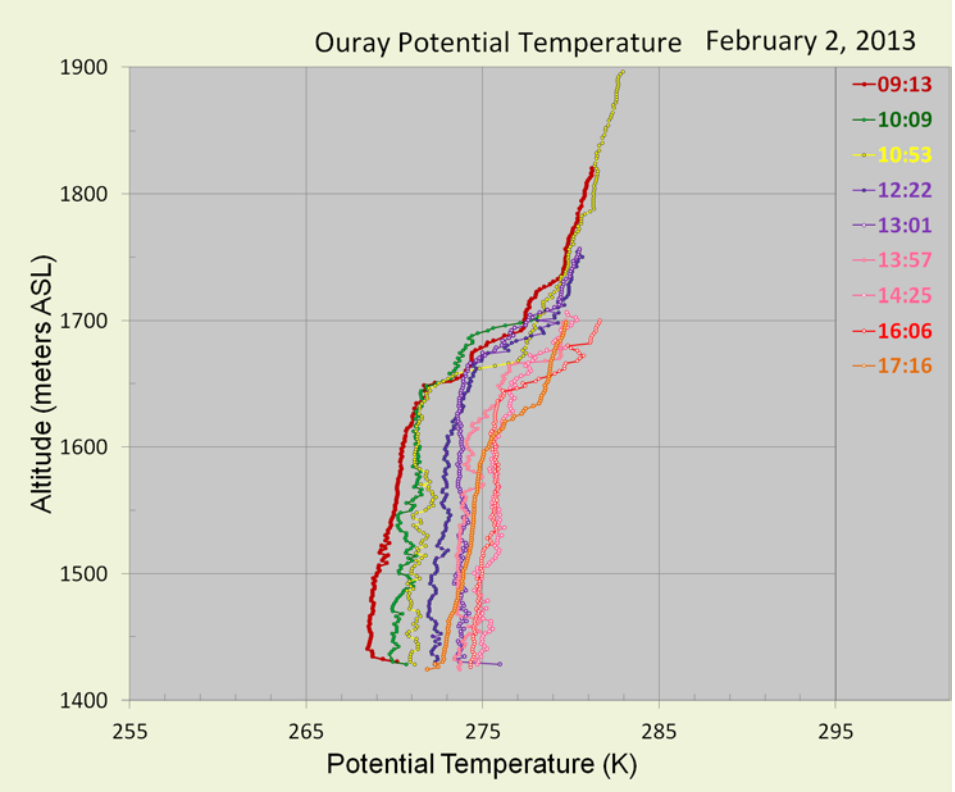

Figure 8-22. (Upper) Ozone did not decrease as much over the night of February 1 as on previous nights and was in the range of 65 ppb in the morning of February 2, rising to 105 ppb by the 17:16 profile. (Lower) The air remained stable with the inversion top rising to 1650 m.

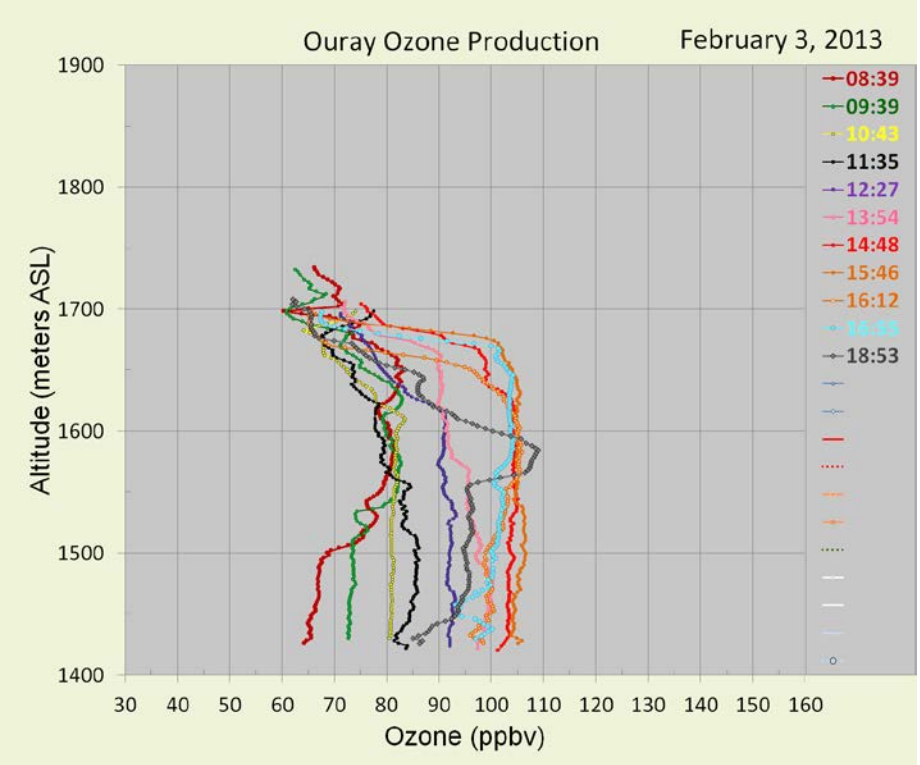

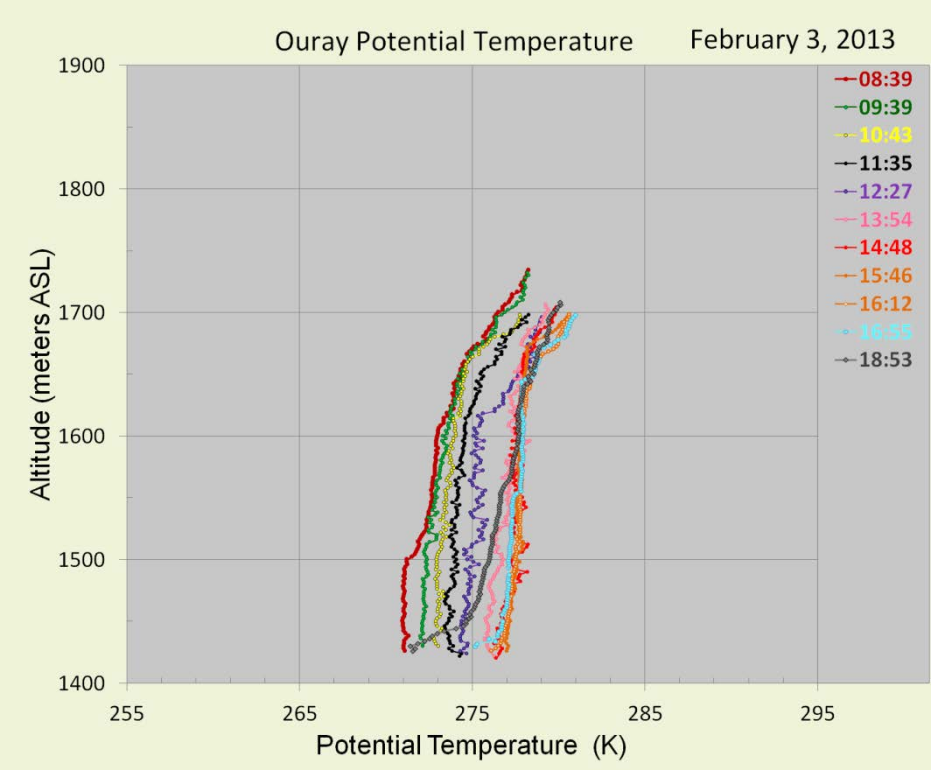

Figure 8-23. (Upper) On February 3, ozone production was similar as on February 2, reaching 105 ppb in the 15:46 profile then decreasing to 85 ppb by 18:53. (Lower) The air remained relatively stable, but the sharp inversion at 1650 m observed on the prior day has somewhat weakened.

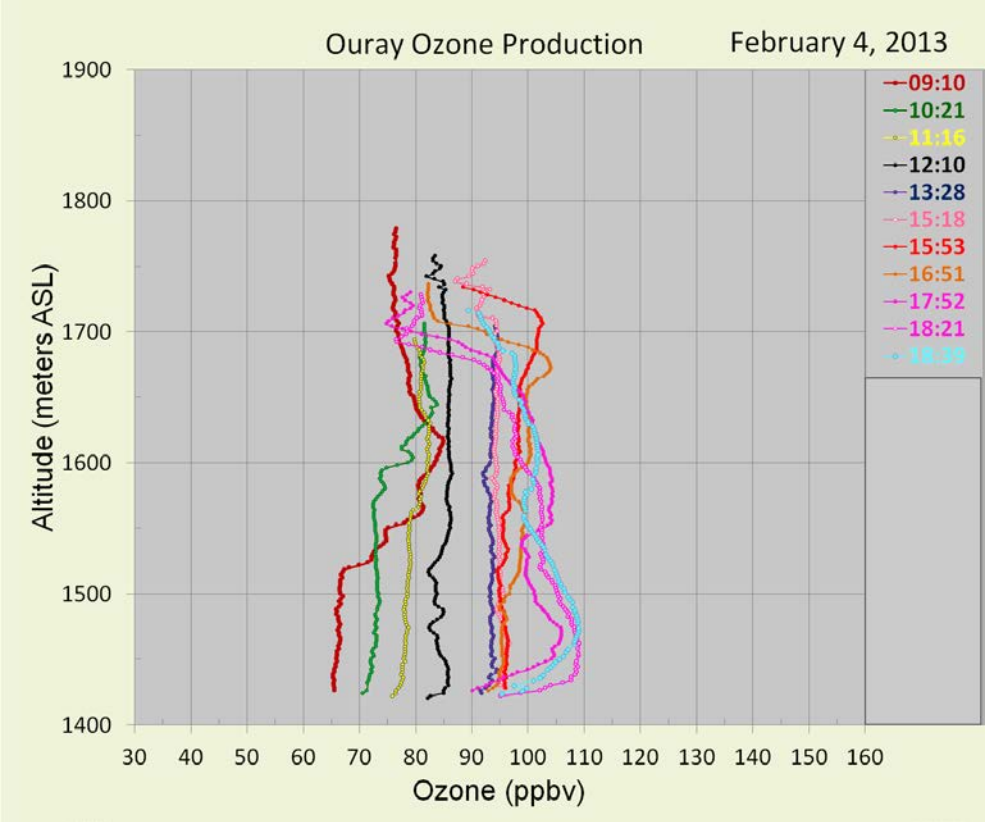

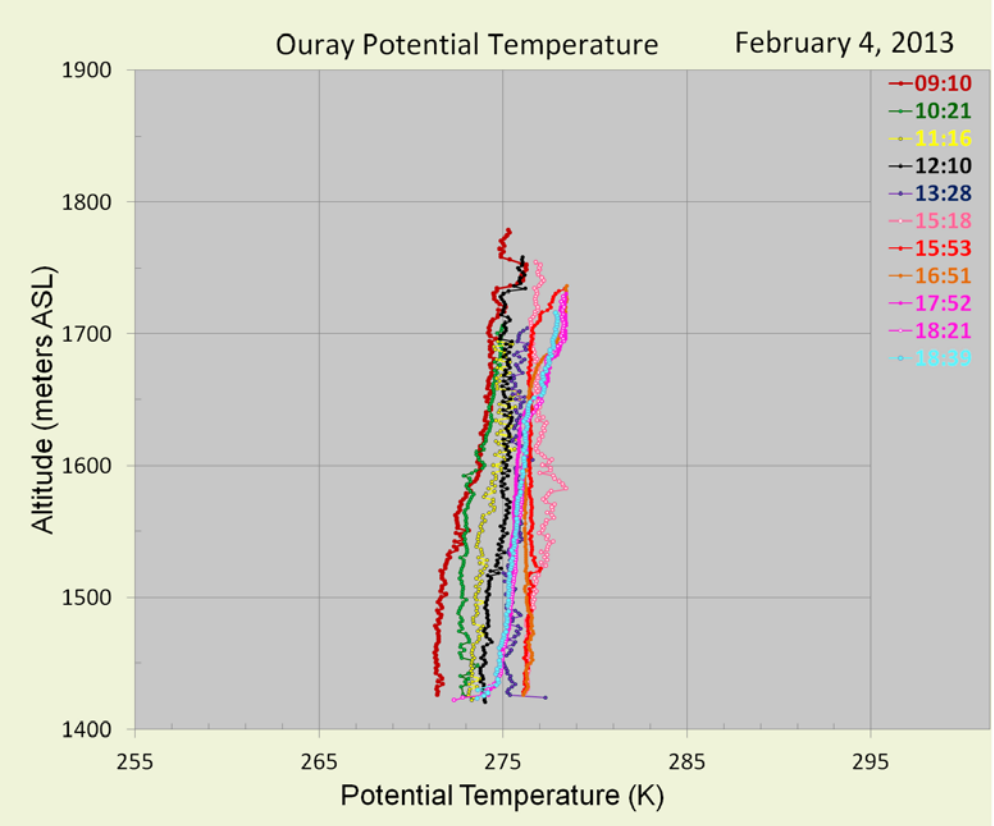

Figure 8-24. (Upper) On February 4, ozone production was similar to that on February 3, but the peak of 110 ppb occurred later in the afternoon at 18:39. (Lower) The air column became better mixed and remained more uniform over the day than earlier in the ozone event.

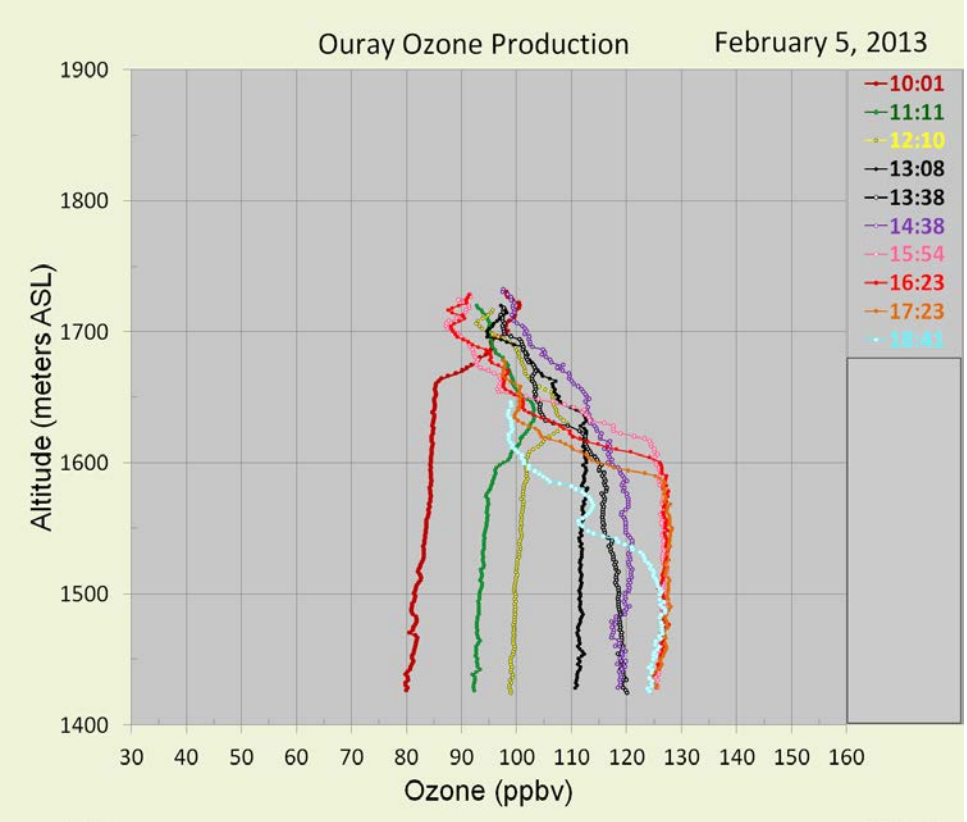

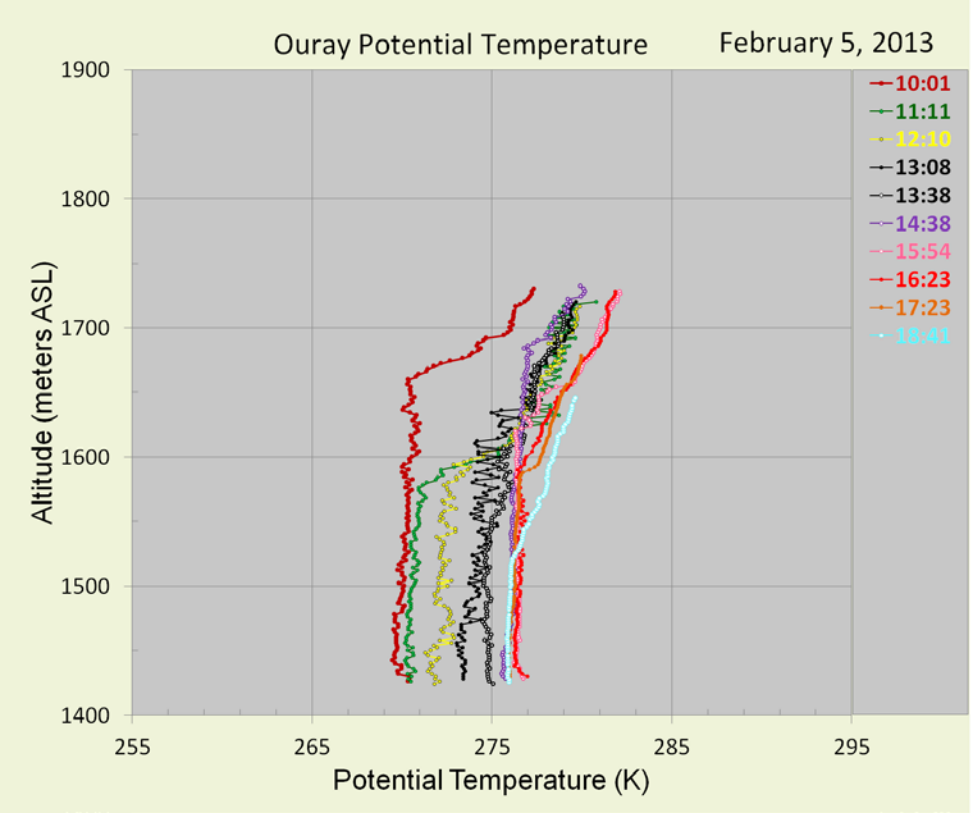

Figure 8-25. (Upper) On February 5 ozone was 80+ ppb in mid-morning increasing to 127 ppb by 16:23 mst before beginning to erode at higher altitudes by 18:41. (Lower) The strong inversion at 1660 m observed in the 10:01 profile lost some of its strength as air warmed and mixed during the day.

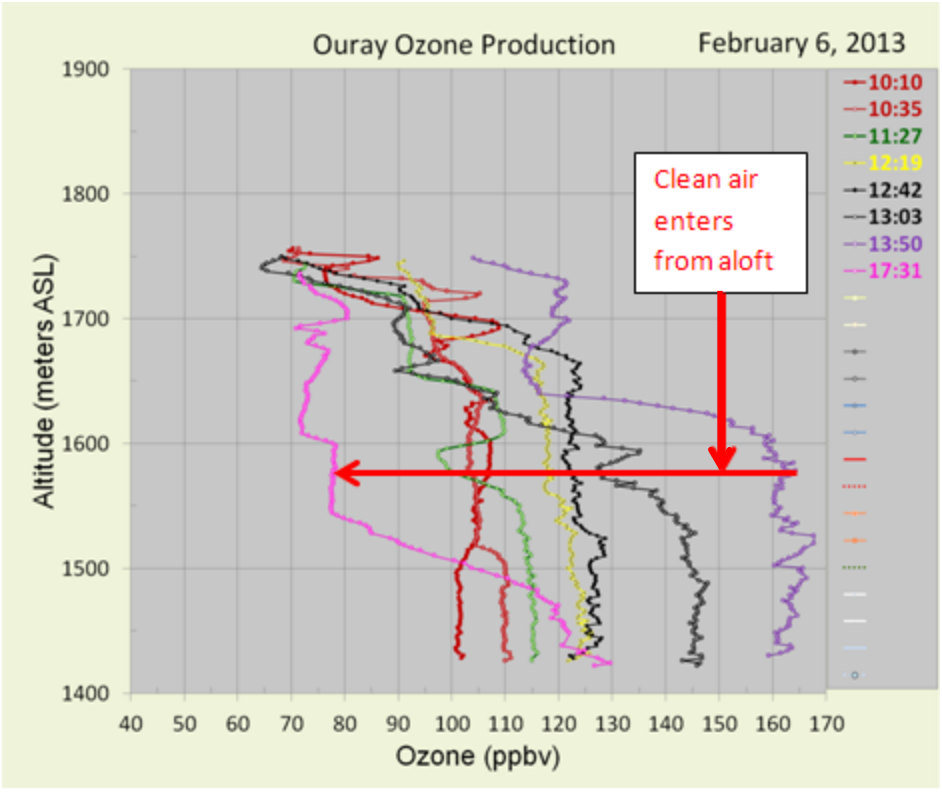

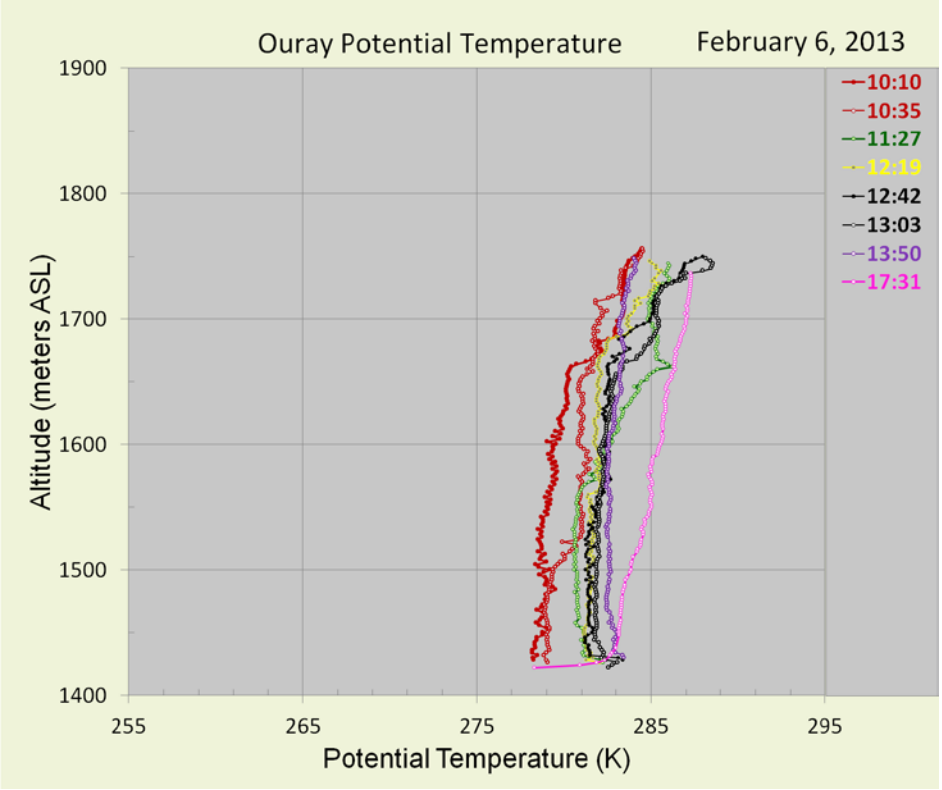

Figure 8-26. (Upper) Ozone remained elevated throughout the night of February 5, with the 10:10 profile showing ozone in the 100+ ppb range. Ozone increased to 165 ppb by 13:50 before rapidly decreasing to the 72-78 ppb range above 15:50 m as clean air moved into the basin from aloft and the west. (Lower) Potential temperature showing the increase in potential temperature at 17:31 as fresh air, now began entering the basin.

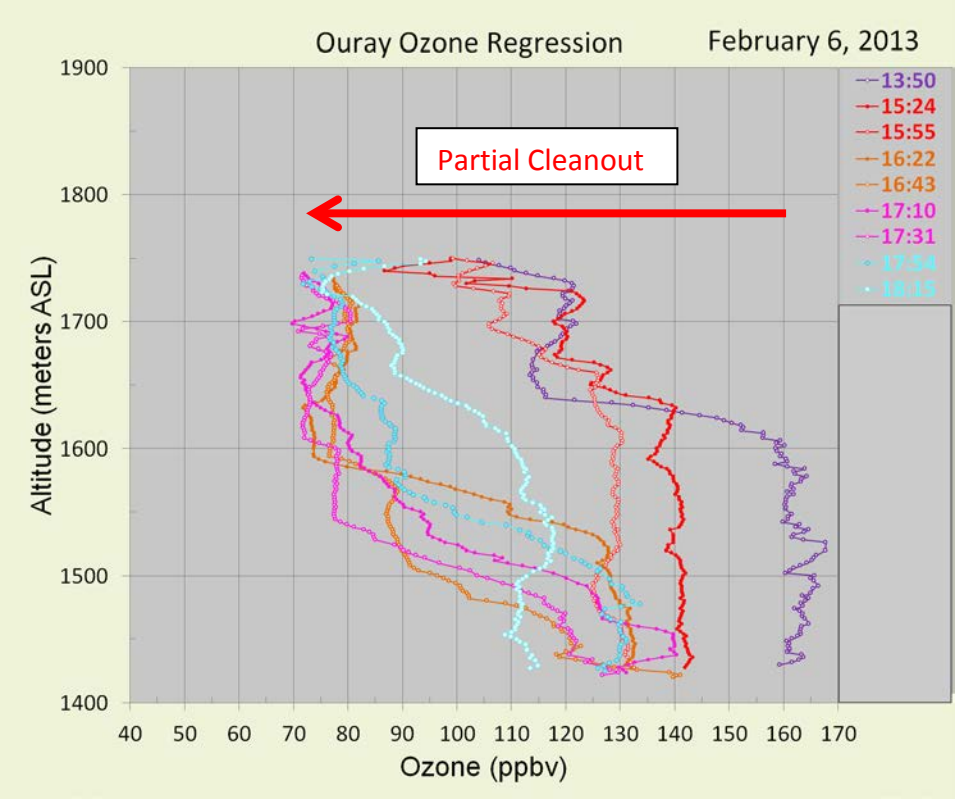

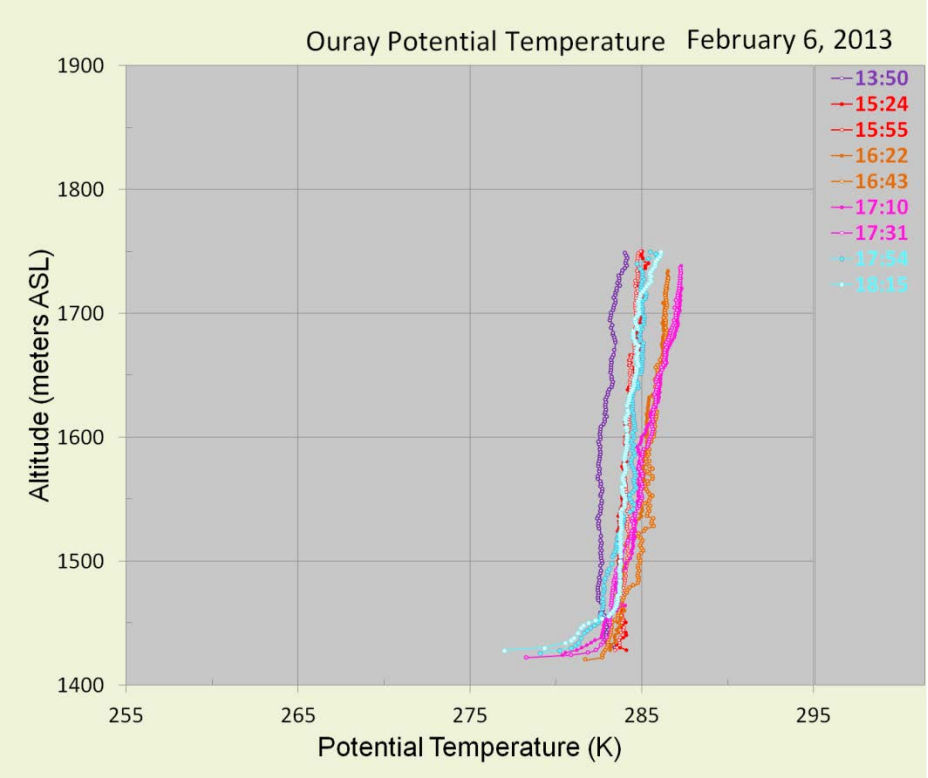

Figure 8-27. (Upper) The profiles for February 6 show the intrusion of cleaner air from aloft from 13:50 to 17:31, then recovery of ozone in the 18:15 profile as ozone rich air sloshes around in the basin. (Lower) Potential temperature remained relatively consistent during the cleanout, but with a strong inversion beginning to develop within a few 10s of meters above the cold, snow covered surface.

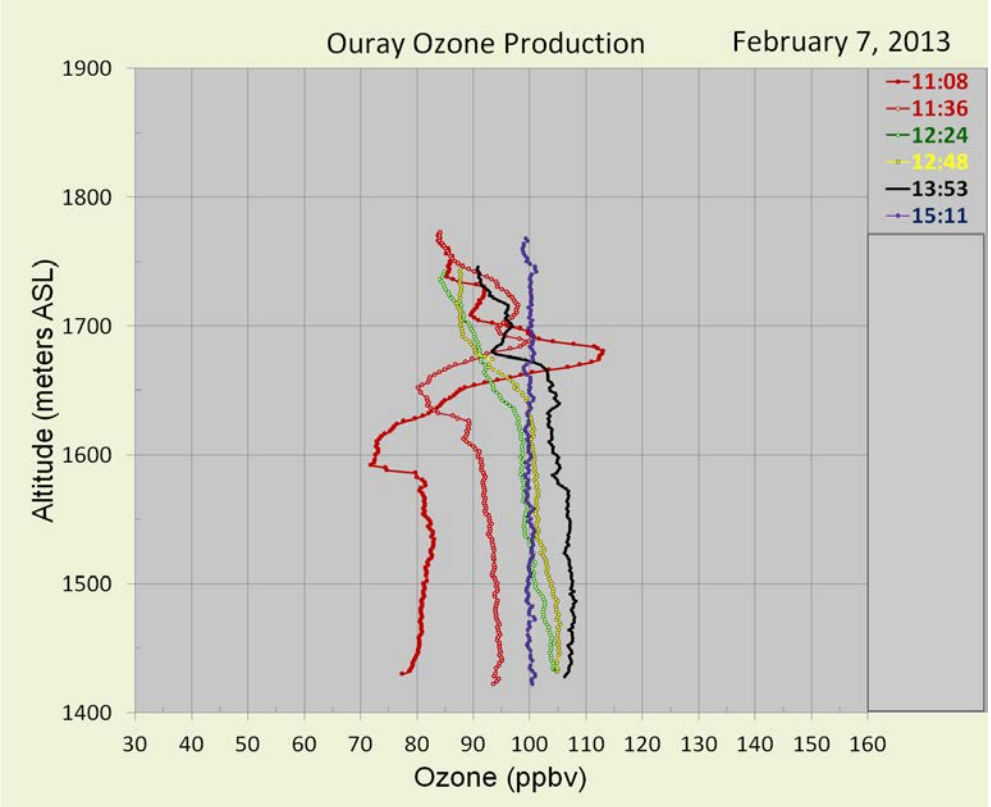

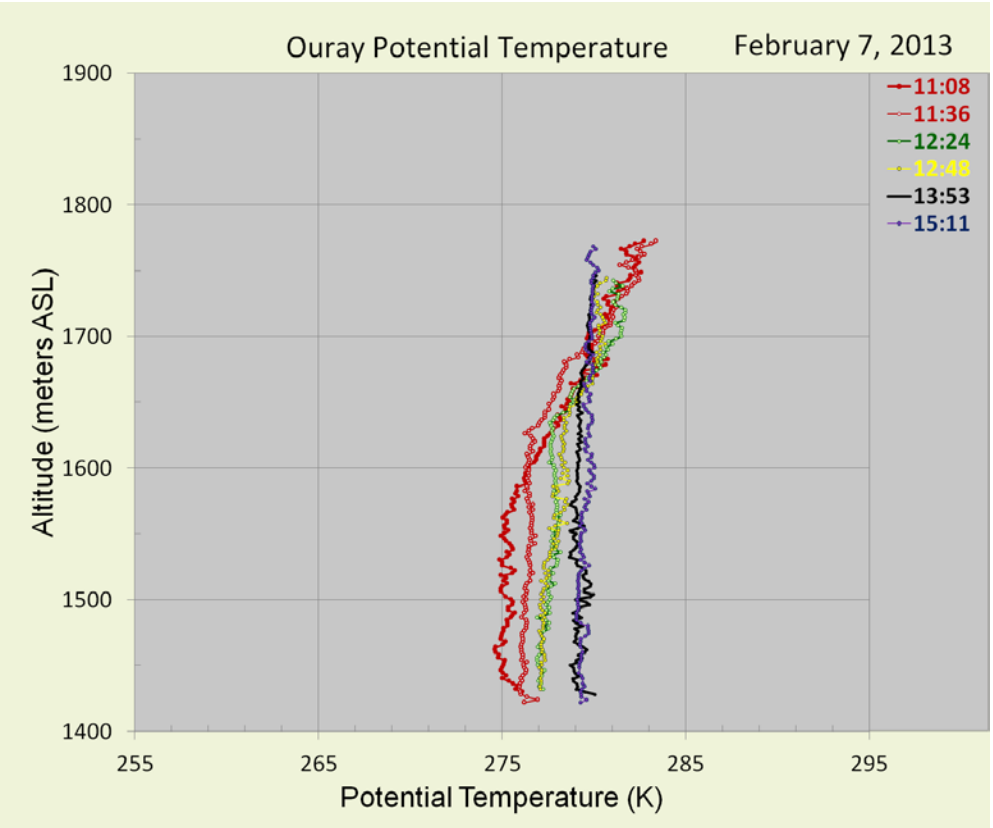

Figure 8-28. (Upper) On February 7 ozone production began again as the prior day's cleanout of the basin was not complete. (Lower) Potential temperatures increased during the day as ozone production also increased.

8.2.3 Free Flying Ozonesonde Profiles

To put the surface ozone and tethersonde measurements into perspective and to be assured that the high concentrations of ozone near the surface were not coming from descending stratospheric air, two free flying ozonesondes were released during the study period. In Figure 8-29 are presented profiles of ozone and temperature from the surface to 11 km on January 25 when surface ozone concentrations were 128 ppb. It is clear that stratospheric air was not contributing to the high surface concentrations. This is also the case for the high surface ozone event of February 7 shown in Figure 8-30. These two profiles were taken during the peaks of two respective high boundary layer ozone events and show that the stratospheric ozone was not coming down from above into the surface inversion. The surface layer ozone was produced at and near the surface. It is also clear that tropospheric air above the shallow, high ozone boundary layer is not the source of the exceptionally high ozone values in the boundary layer. The free troposphere ozone profile concentrations were similar in 2012 and 2013.

8.2.4 Mobile Surface Ozone Measurements

Each day of the study period, the NOAA crew measured ozone concentrations while driving from and returning to Vernal from tethersonde sites in the basin. On other days, mobile measurements were conducted east and south past Bonanza power plant and on one day through the basin and south up the mountain slope that carried the van above the temperature inversion and high ozone concentration layer. The configuration of the ozonesonde mounted on a NOAA van is presented in Figure 8-31. During the drives through the basin, the mobile van passed near the Red Wash and Ouray EPA and the Ouray Wildlife ozone monitors. Ozone measurements from the mobile ozonesonde and fixed sites are presented in Figure 8-33 where it may be observed that there was excellent agreement considering the difference in distance between the relative measurement sites and the fact the mobile van occasionally operated in excess of 60 mph when passing the fixed sites at distances of up to a mile.

Data from a drive around the basin during the February 6 ozone event is presented in Figure 8-32 for surface ozone concentrations plotted aganst elevation above sea level over time. From this figure it can be seen that ozone concentrations were in the 75 ppb range when leaving Vernal, rising to 115 ppb then decreasing to 90 ppb at Red Wash (point 3) as the elevation of the road was high enough (1720 m) that the van was beginning to poke through the top of the inversion layer. When the elevation of the road decreased, ozone concentrations increased to 120 ppb near Fantasy Canyon (point 5) and Horsepool (point 6). At Point 7, near the Ouray EPA site, surface ozone was 140 ppb. Driving up the south rim of the basin, ozone began to decrease at 1650 m as the van ascended through the base of the inversion layer, decreasing to backgrond ozone concentration of 50 ppb at 2000 m. The pattern was repeated in reverse on the descent. High ozone beneath the inversion and background concentrations above the inversion layer were consistently observed in the tethersonde and aircraft data. Graphs from the other days' drives are available at:
ftp://ftp.cmdl.noaa.gov/ozwv/ozone/Uintah_2013_Tether_OzoneSondes/ .

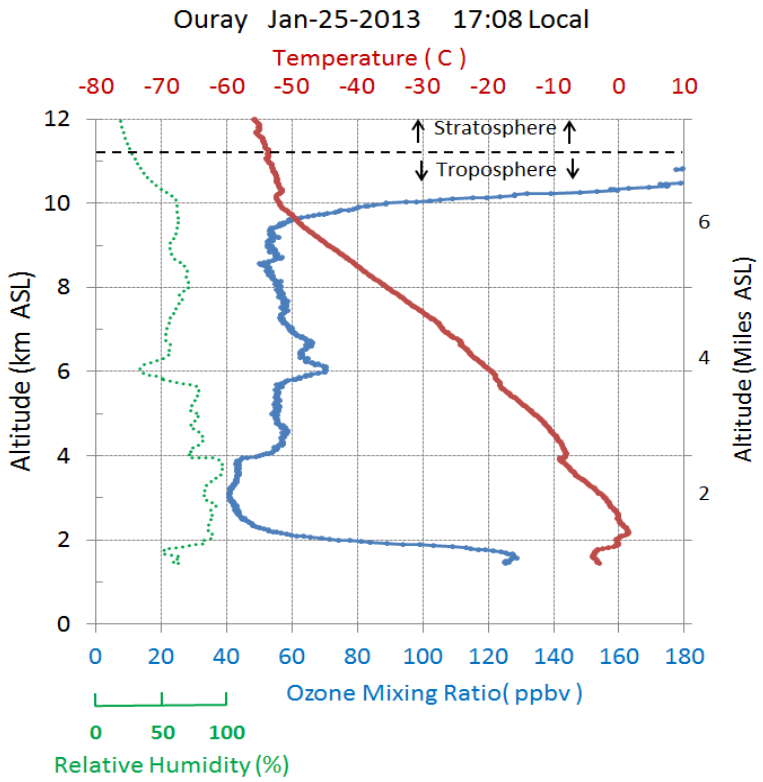

Figure 8-29. Free flying ozonesonde released from the Ouray Wildlife Refuge when ozone in the boundary layer was in excess of 120 ppb, January 25, 2013. Note the shallow elevated ozone layer near the surface, background ozone concentrations from 3 km to 9.5 km and then stratospheric ozone concentrations exceeding 180 ppb above 10 km.

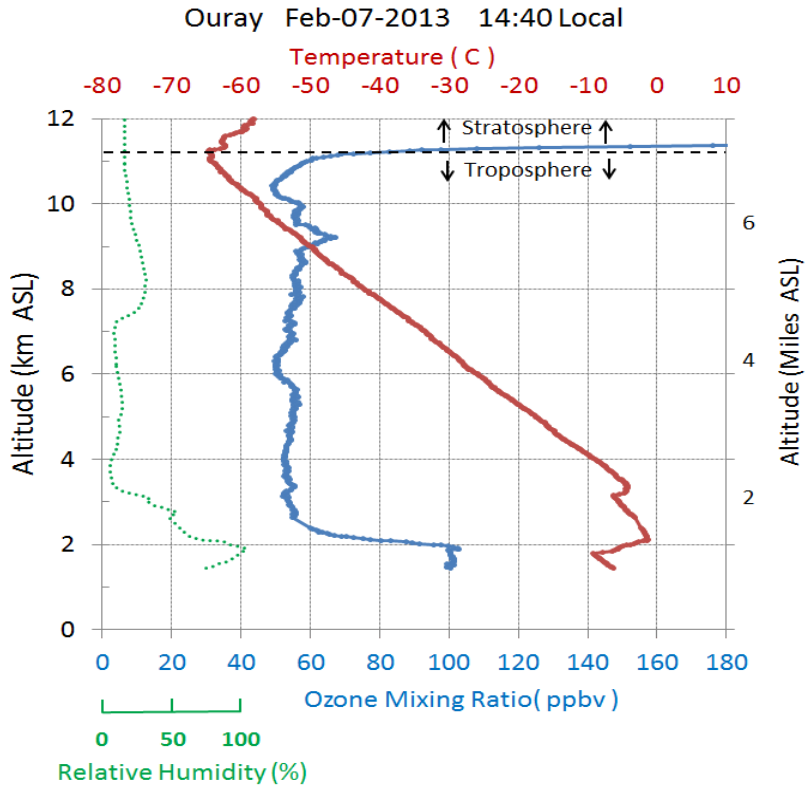

Figure 8-30. Free flying ozonesonde released from the Ouray Wildlife Refuge when ozone in the boundary layer was 100 ppb, February 7, 2013. Note the shallow elevated ozone layer near the surface, background concentrations from 2 km to 11.5 km and then stratospheric ozone concentrations exceeding 180 ppb above that level.

Figure 8-31. Ozonesondes mounted in the window of a NOAA van used to measure ozone concentrations while driving around the Uinta Basin. This photo was taken during the 2012 study but a similar configuration was used in 2013.

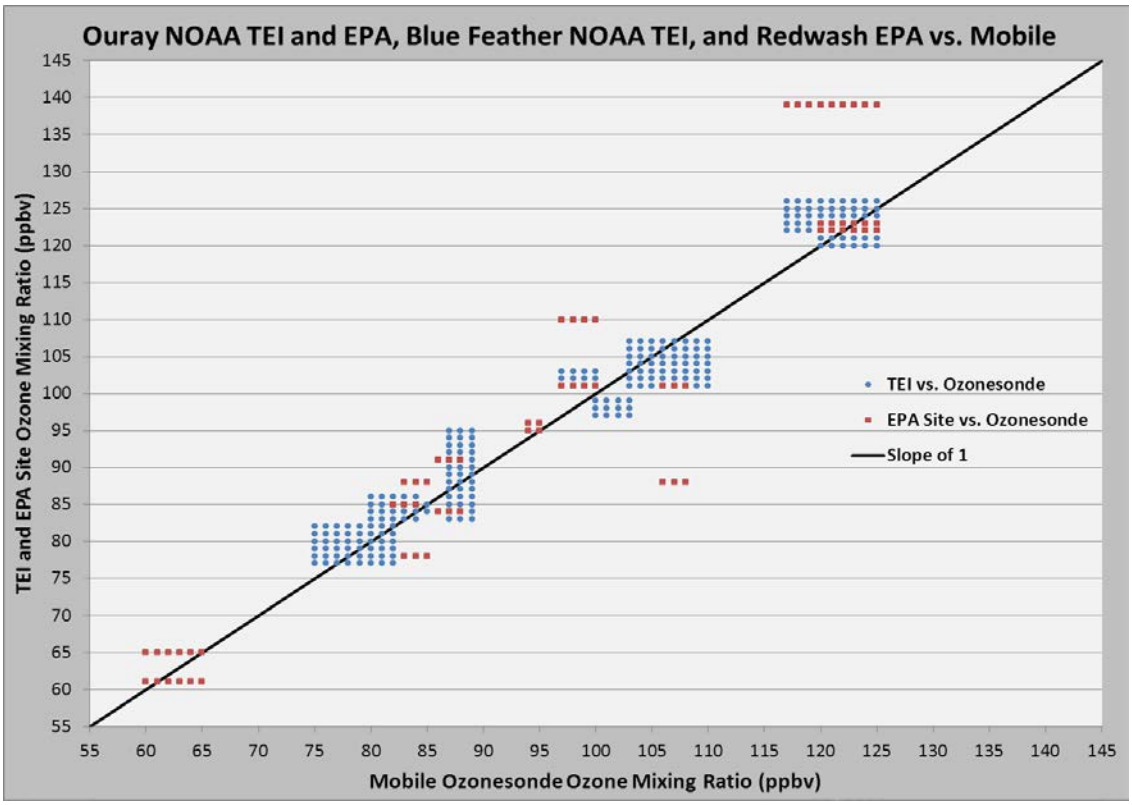

Figure 8-32. Comparison between the mobile ozonesonde operated on the side of a NOAA van and fixed ozone measurements when the van passed near (up to a mile difference) the Red Wash and Ouray EPA ozone monitors and the NOAA monitor at the Ouray Wildlife Refuge. Considering the timing, difference in distance and the fact the mobile van occasionally operated in excess of 60 mph when passing the fixed sites, the agreement is excellent.

Mobile Ozone Measurements, Feb 6, 2013

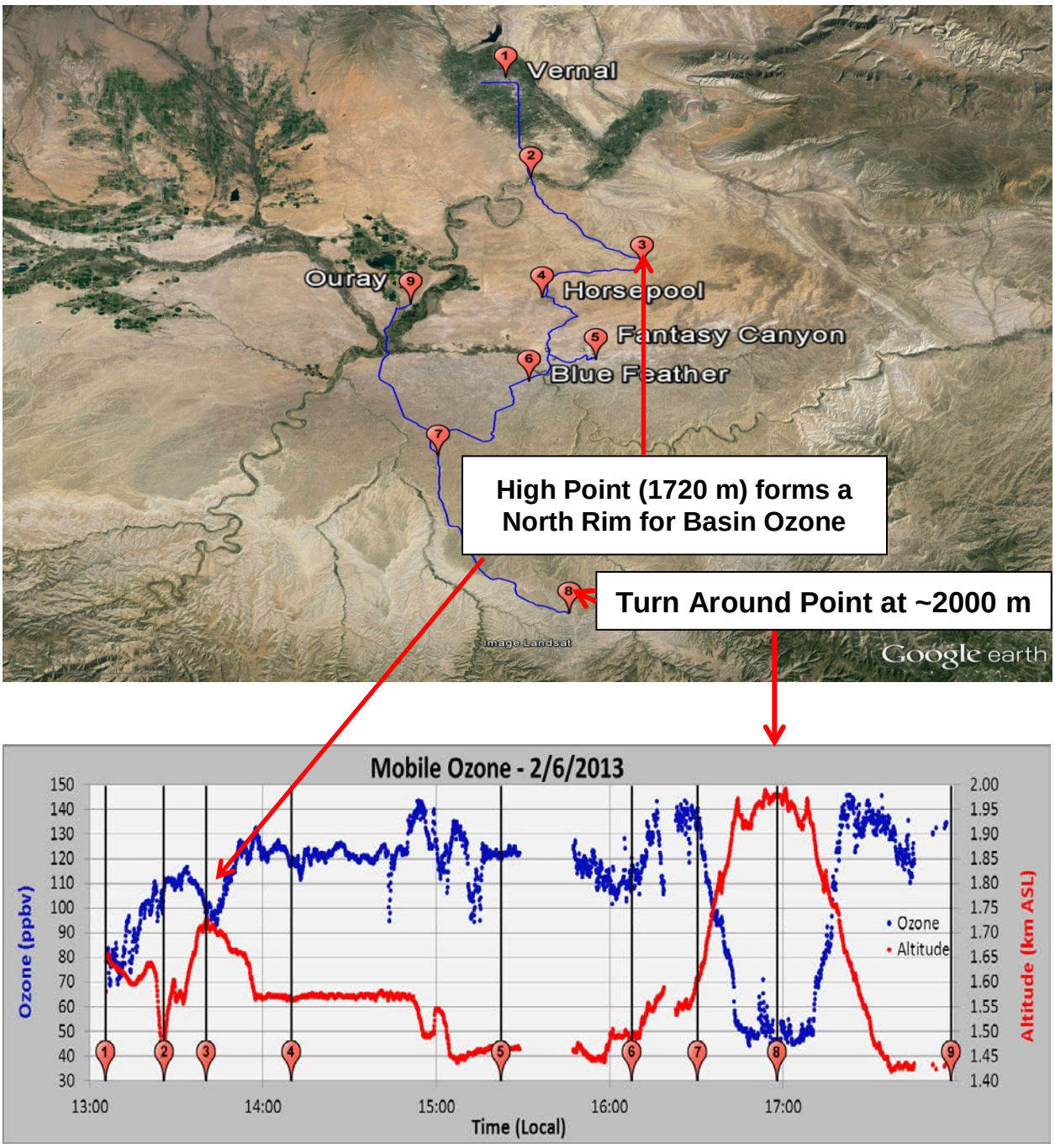

Figure 8-33. Surface ozone concentrations plotted aganst altitude on a drive beginning in Vernal then through the eastern portion of the Uinta Basin, February 6, 2013. Note the the decrease in ozone (point 3) at 1720 m crossing the ridge near Red Wash, and the large ozone decrease as the van began to ascend through the inversion layer at 1720 m (Point 7) and the increase in ozone as the van descended back into the top of inversion layer after turning around at ~2,000 m (Point 8).

8.2.5 Contour Plots of Ozone Structure during Ozone Production and Cleanout Events

Contour plots of ozone concentrations measured with tethersondes plotted by altitude and time are presented in Figures 8-34 through 8-40 for January 26 - February 6, 2013. On some days up to 22 separate tethersonde profiles were used to produce the contours. In Figure 34 may be seen the final day of a peak ozone event confined to a 150-200 m deep layer that topped out in the 1650-1700 m altitude. Figure 8-35 shows the middle stage of the subsequent cleanout produced by fresh air from the west mixing into the basin. Figure 8-36 shows that once the basin had been flushed out the incoming air contained background ozone concentrations. By January 31 (Figure 8-37), stagnation had redeveloped in the basin and local effluents from gas and oil operations began providing precursor gases for ozone formation. Ozone production continued through to February 6 (Figures 8-38, 8-39 and 8-40). On February 7 a partial cleanout of the basin began. The tethersonde operations were completed on the afternoon of February 7.

One of the most notable features of the ozone profile measurements is the vertical development of ozone production each day. Ozone production does not begin solely in a shallow layer next to the surface, but proceeds through the entire layer below the temperature inversion as indicated by the potential temperature profile (see Figures 8-18 - 8-24). As the inversion layer expands vertically with increasing temperature from solar heating, the ozone production layer grows vertically as well. This leads to nearly constant ozone mixing ratios in this thermally mixed layer. The mixing is, however, not so strong that the layer does not remain capped.

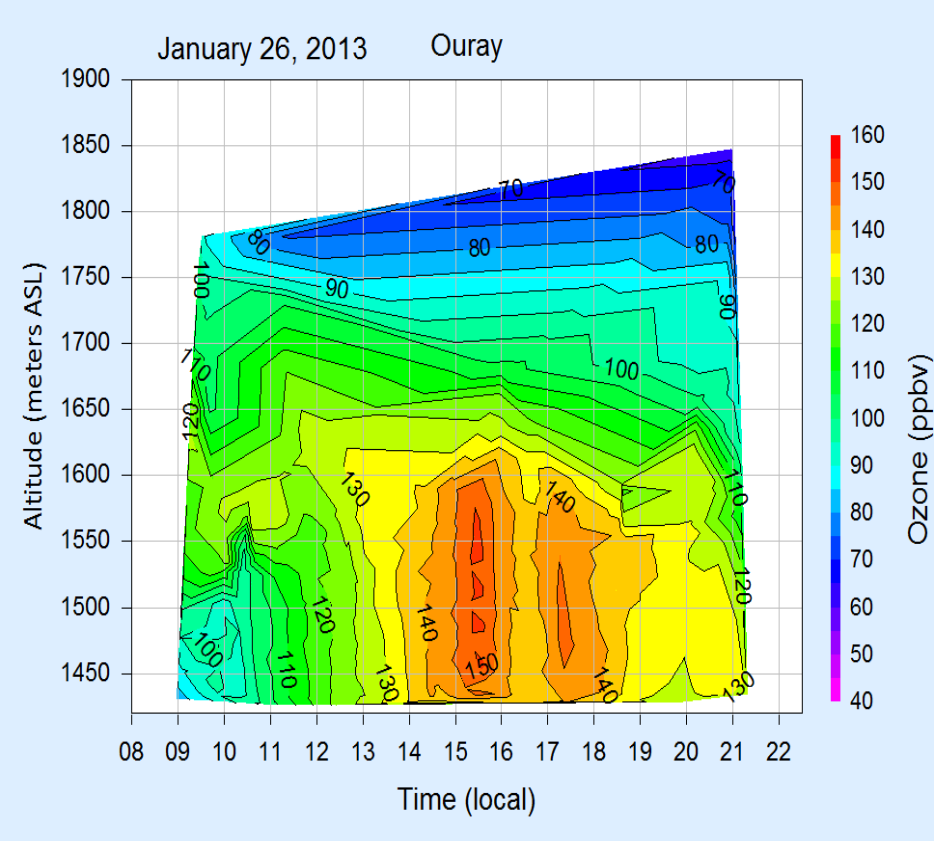

Figure 8-34. Contour plot of ozone concentrations above the Ouray Wildlife Refuge in the first ozone event presented in Figure 8-9. Note that high concentrations of ozone occur in mid-afternoon and are concentrated between the surface and 1600 m altitude.

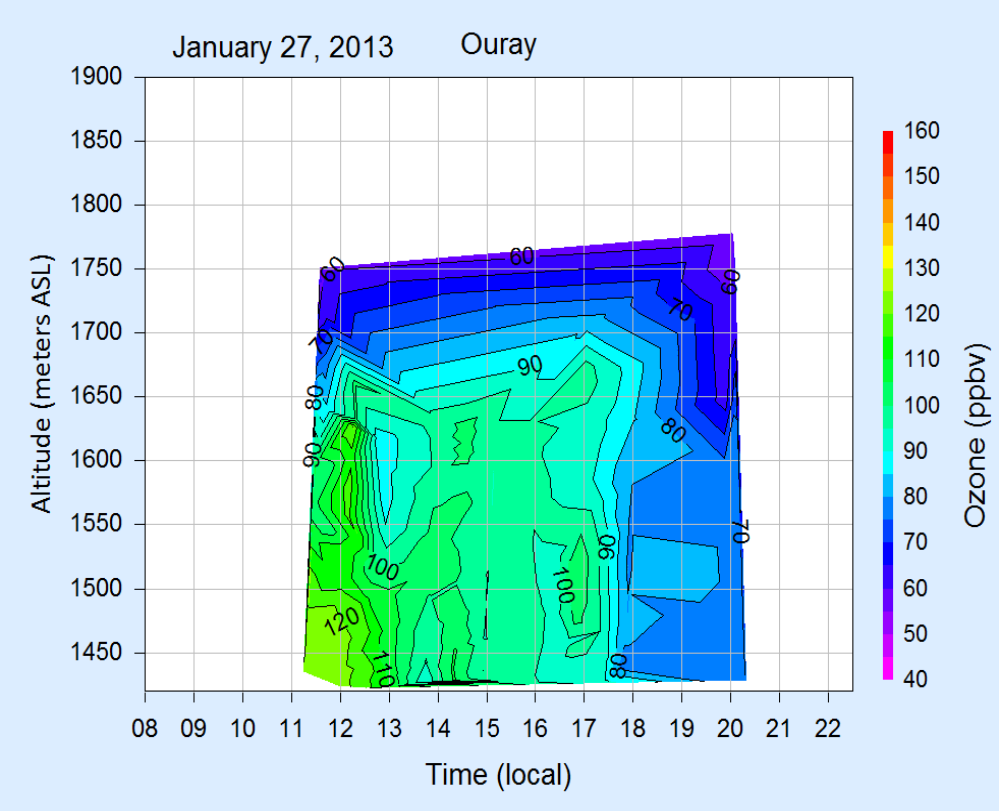

Figure 8-35. Contour plot of ozone concentrations above the Ouray Wildlife Refuge showing the beginning of the basin-wide cleanout that began the evening of January 27.

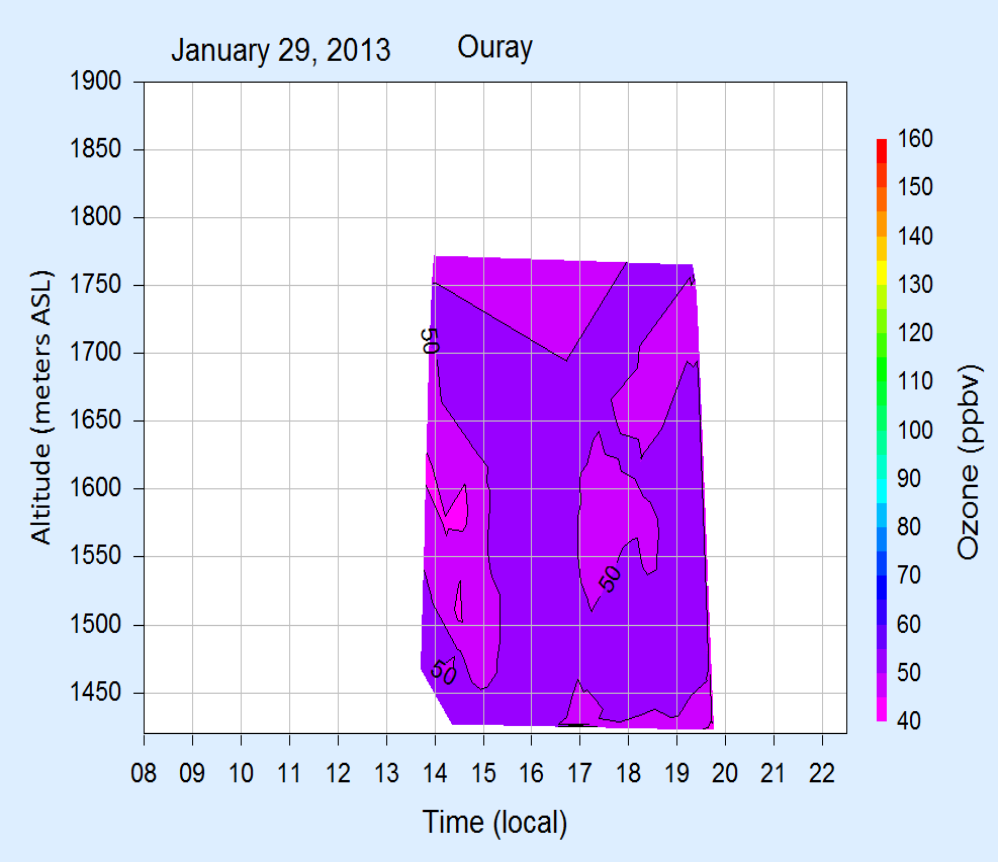

Figure 8-36. Contour plot of ozone concentrations above the Ouray Wildlife Refuge the day the cleanout was essentially completed on January 29. Ozone concentrations of less than 50 ppb are considered background in this location and season.

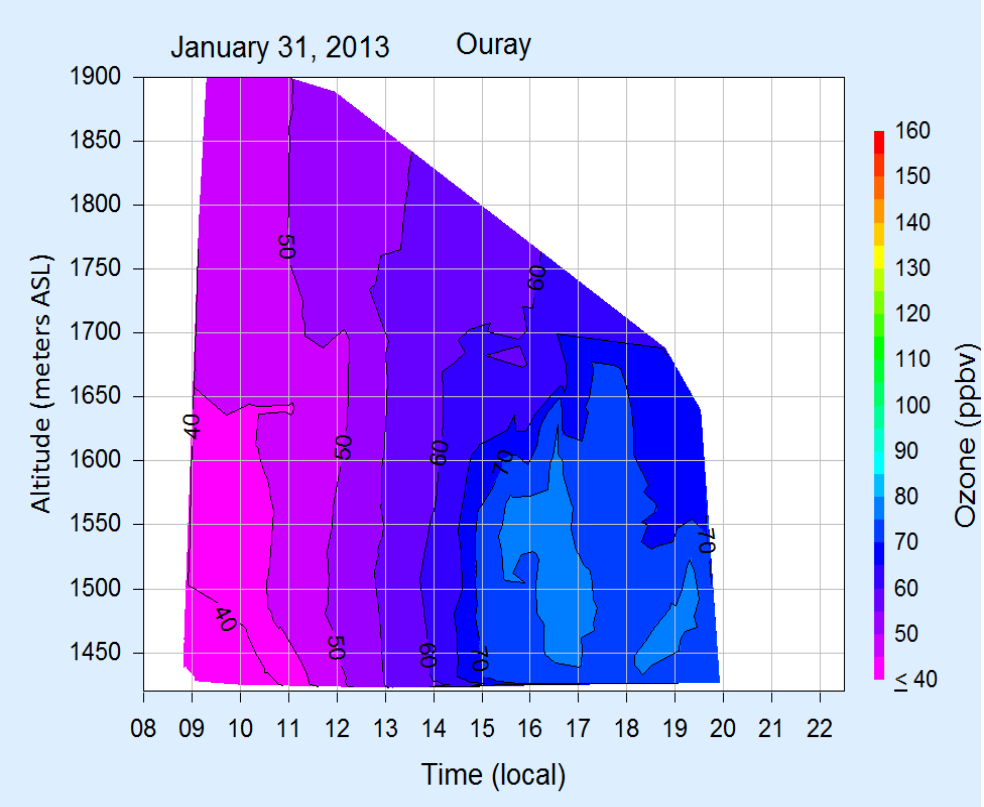

Figure 8-37. Contour plot of ozone concentrations above the Ouray Wildlife Refuge showing the beginning of the next ozone event. This event was also the focus of the NOAA aircraft flights.

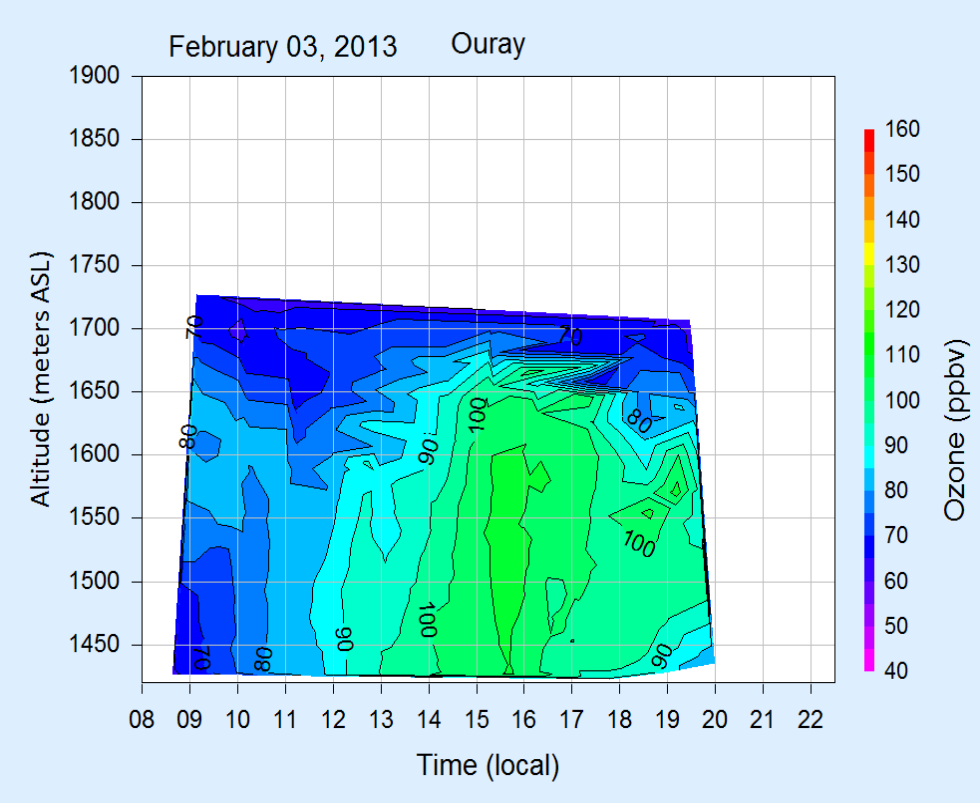

Figure 8-38. Contour plot of ozone concentrations above the Ouray Wildlife Refuge showing the production of ozone now in excess of 100 ppb leading up to the peak on February 6.

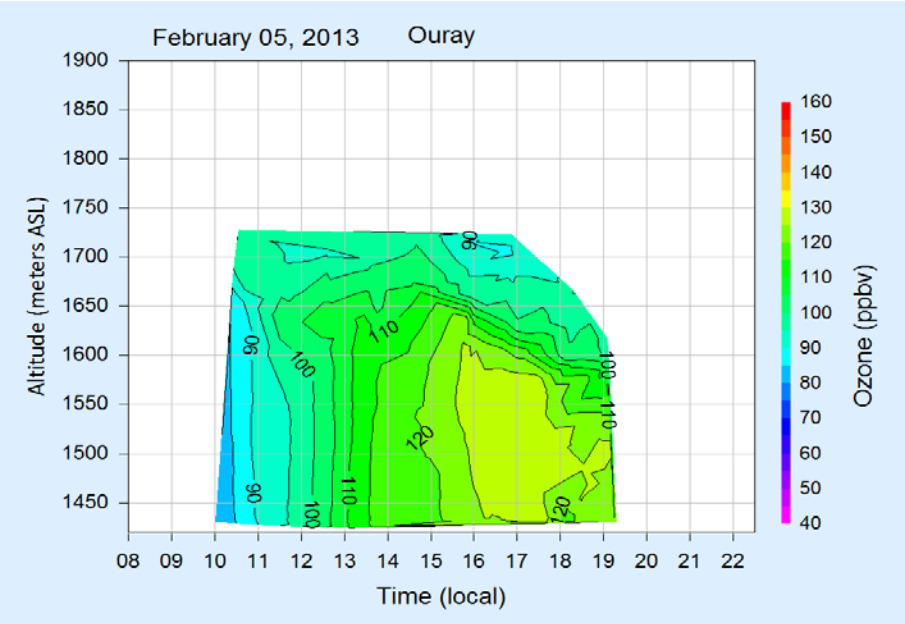

Figure 8-39. Contour plot of ozone concentrations above the Ouray Wildlife Refuge the day prior to the peak of the basin wide ozone event. Note the high ozone concentrations in excess of 125 ppb in the late afternoon.

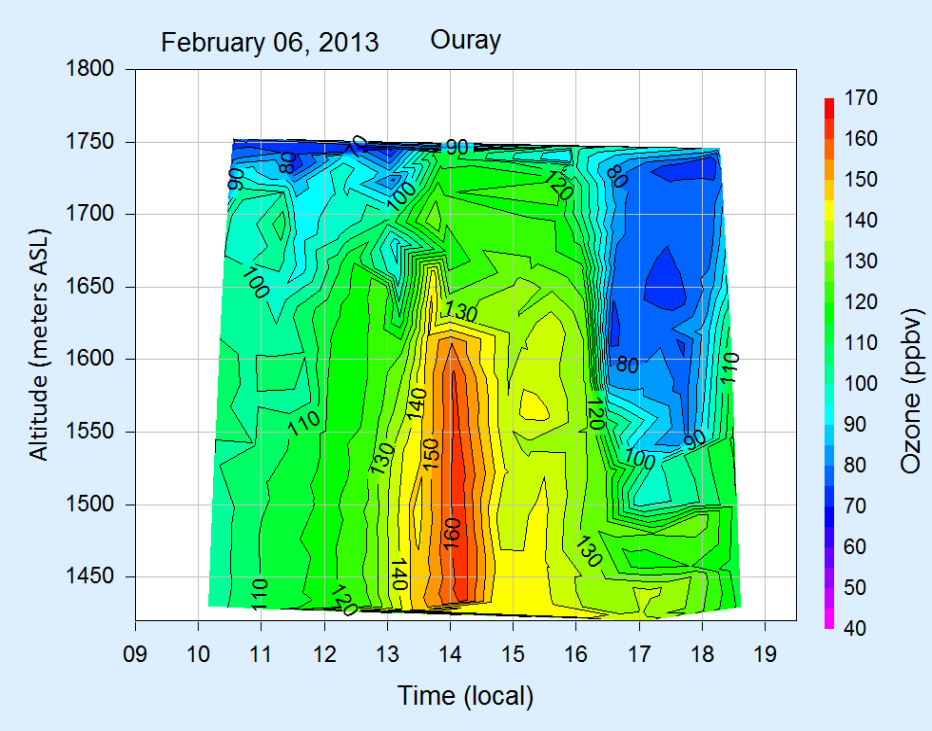

Figure 8-40. Contour plot of ozone concentrations above the Ouray Wildlife Refuge at the peak of the basin wide ozone event. Later in the day air from the west began a partial basin cleanout as may be seen in the low ozone concentration air descending into the basin beginning around 1600 (blue area) down to 1550 m.

8.2.6 Ozone Mixing Out of the Boundary Layer

Above the strong ozone production layer with a top at ~1650 m is a strong gradient layer that extends to ~1800 m (Figures 8-34 and 8-40) where tropospheric background ozone levels are encountered. This gradient layer suggests that some ozone (and likely other constituents) are mixed out of the ozone production layer into the overlaying troposphere even during the times with a capping inversion layer over the basin.

8.2.7 Contours of Two Ozone Production Events and the Intervening Cleanout.

A contour plot of ozone concentrations above Ouray January 24 - February 7 is presented in Figure 8-41. Two high ozone events (orange-red contours) and a cleanout separating the events (blue contours) are clearly seen.

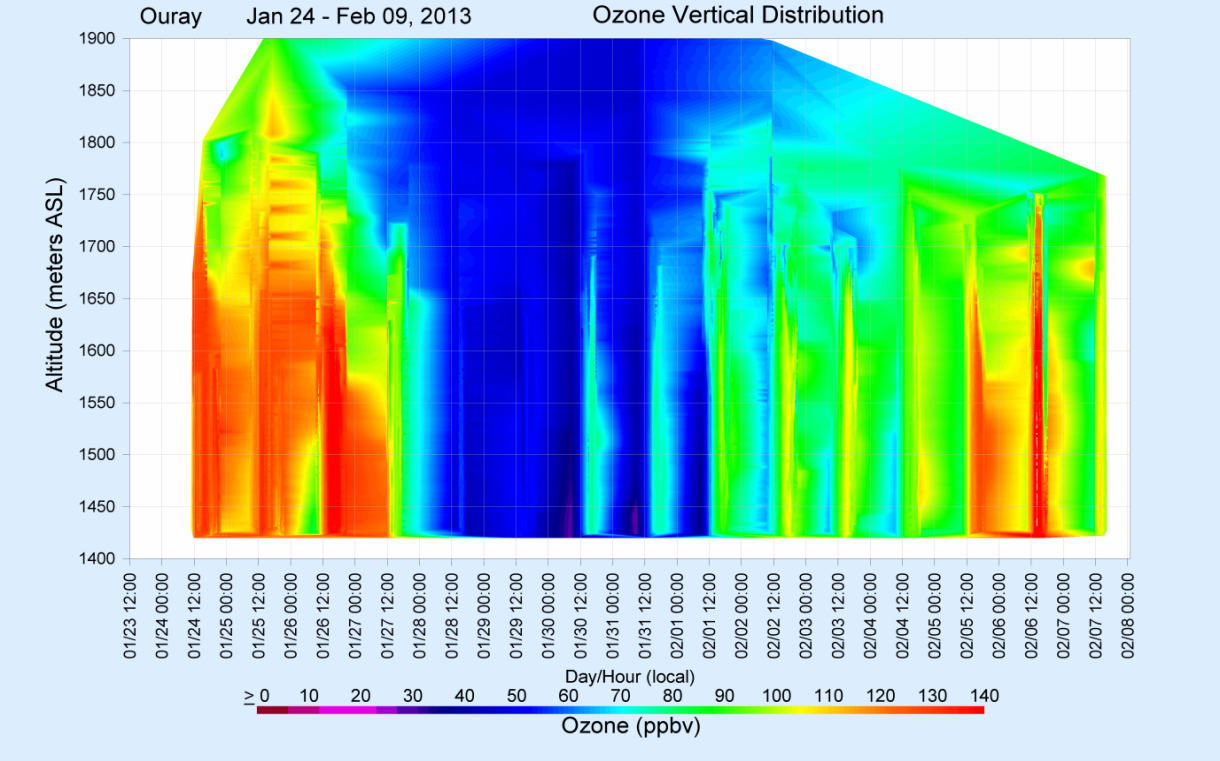

Figure 8-41. Contour plot of ozone concentrations above the Ouray Wildlife Refuge January 24 - February 7 showing the ozone event ending January 27 and the cleanout that lasted from January 27 to the beginning of the new ozone production event in early February. That event peaked on February 6.

8.3 Did the Bonanza Power Plant Contribute to Ozone Precursors in Winter 2013?

Bonanza power plant is located on the eastern edge of the Uinta gas field and questions as to the possibility of the plant contributing to ozone precursors (mostly NO_x) involved in the wintertime photochemical ozone production have been raised. During the 2013 Uintah ozone study, a wide variety of balloon borne, aircraft and remote sensing measurements were undertaken to address the question. In short, there is no evidence that the Bonanza power plant plume contributes significant amounts of precursors in the inversion layer and is therefore not likely a major driver of the wintertime high ozone events in the winter of 2013. The basis for this statement is presented below.

8.3.1 Aircraft Measurements in the Bonanza Power Plant Plume

Figure 8-42 is a photo of the Bonanza power plant plume and the water vapor condensate from the surface cooling ponds. The top of the power plant stack is at an elevation of 1715.8 m. Due to the relative warmth of the plume exhaust in winter, the plume generally rises an additional 2 to 3 stack heights before reaching neutral buoyancy at between 1900 and 2200 m. The inversion height in 2013 was in the 1600 to 1750 m range, well below the plume heights.

Figure 8-43 is a photo of the Bonanza power plant plume taken from the NOAA research aircraft on February 2, 2013 showing the top of the ozone rich surface layer and the power plant plume rising above the inversion. The plume eventually reaches neutral buoyancy at an altitude of about 1900 m. On this day that is 300 m above the top of the photochemical ozone production layer contained beneath the temperature inversion.

On February 2 and 5, 2013 the aircraft spent portions of the flights studying the altitude and dispersion of the power plant plume. Profiles were conducted near the plant, over Horsepool and westward across the basin as easterly winds carried the plume across the basin. In the aircraft section of this report, Figure 8-17, profile 4, shows the power plant plume to be centered at just less than 1900 m. Profiles through the plume on February 5 (aircraft section, Figure 8-19, profiles 1 and 3) also show the power plant plume at 1900 m.

Figure 8-42. Bonanza power plant with buoyant exhaust plume and water vapor from the cooling ponds. The top of the stack is 1715.8 m and the plume generally rose an additional 2 to 3 stack heights before leveling out in the 1900 to 2200 m range. In the winter of 2013 the inversion top was generally between 1600 and 1750 m.

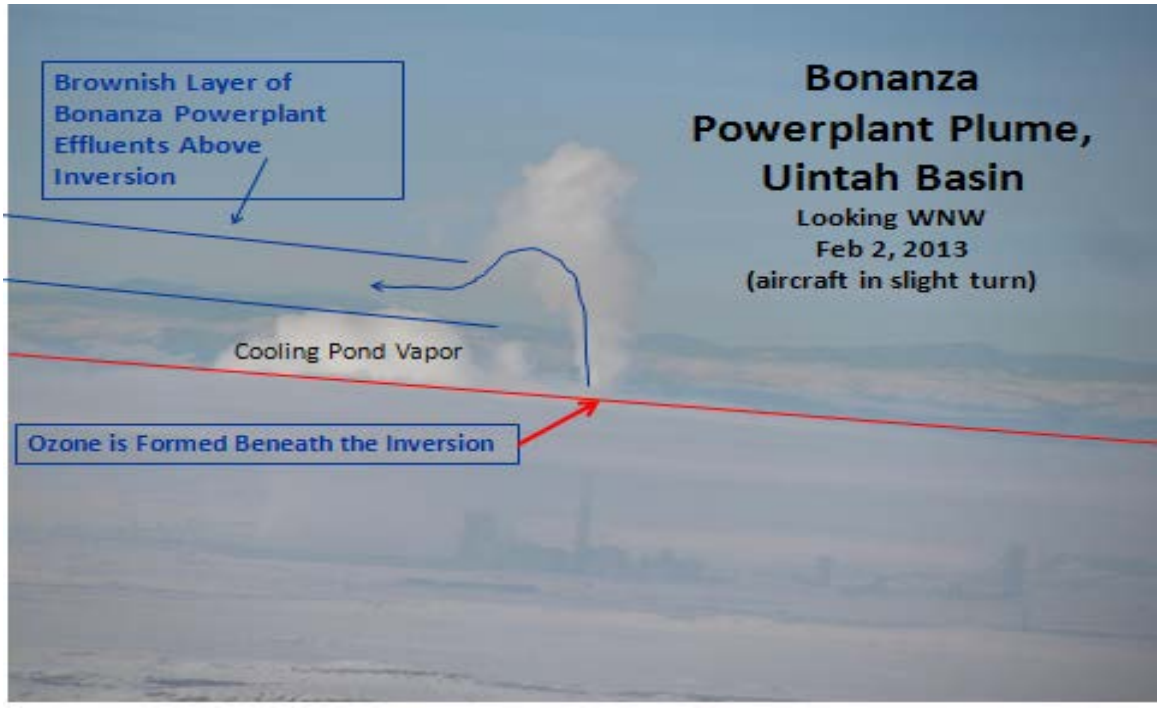

Figure 8-43. Bonanza power plant plume rising well above the inversion layer at 1600 m before achieving neutral buoyancy and streaming westward out over the basin at 1900 m. Photograph by Colm Sweeney, airborne scientist, CIRES/NOAA.

8.3.2 Horsepool Tethersonde Measurements of the Bonanza Power Plant Plume

The ozonesondes used in this study indicate low ozone concentrations in the presence of high sulfur dioxide (SO_2) concentrations observed in power plant plumes. In addition, when the ozonesondes are in power plant plumes, titration of the background ozone by NO_x removes ozone. The net result of these two processes is zones of low or no ozone when the ozonesondes were in the Bonanza power plant plume. The tethersonde at Ouray was operated such that the maximum altitudes of the ascending profiles were determined by reaching the top of the enhanced ozone layer, at which point the tethersondes were put into descent mode. Thus, the tethersondes from the Ouray site was never high enough to enter the Bonanza power plant plume. On a few occasions, the Fantasy Canyon tethersonde was allowed to rise into the plume. The Horsepool tethersonde operated by the INSTAAR group was operated to much higher altitudes and regularly passed through the power plant plume when it was present over Horsepool. The Horsepool site is 17 km from the Bonanza power plant.

Figures 8-44 through 8-47 show representative measurements in the Bonanza power plant plume above the Horsepool site over a 12 day period. A composite ozone cross section with plumes annotated is presented in Figure 8-48 where it may be seen that Bonanza power plant plumes were at the 1900-2000 m level when over Horsepool except on the night of February 14 during the cleanout when the plume was probably pushed down 100-150 m by the fresh air descending into the basin.

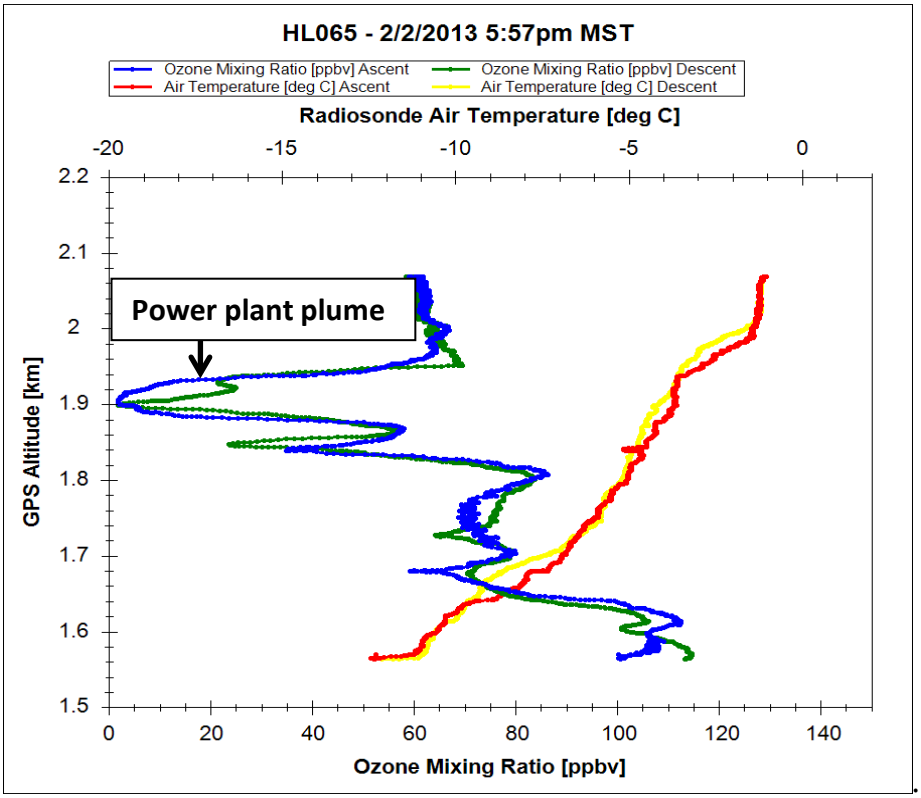

Figure 8-44. Horsepool ozone and temperature profiles on February 2, 2013 showing the elevated ozone layer capped at 1620 m and the power plant plume at 1900 m. The time is the beginning of the balloon ascent that generally lasted from 30 to 45 minutes.

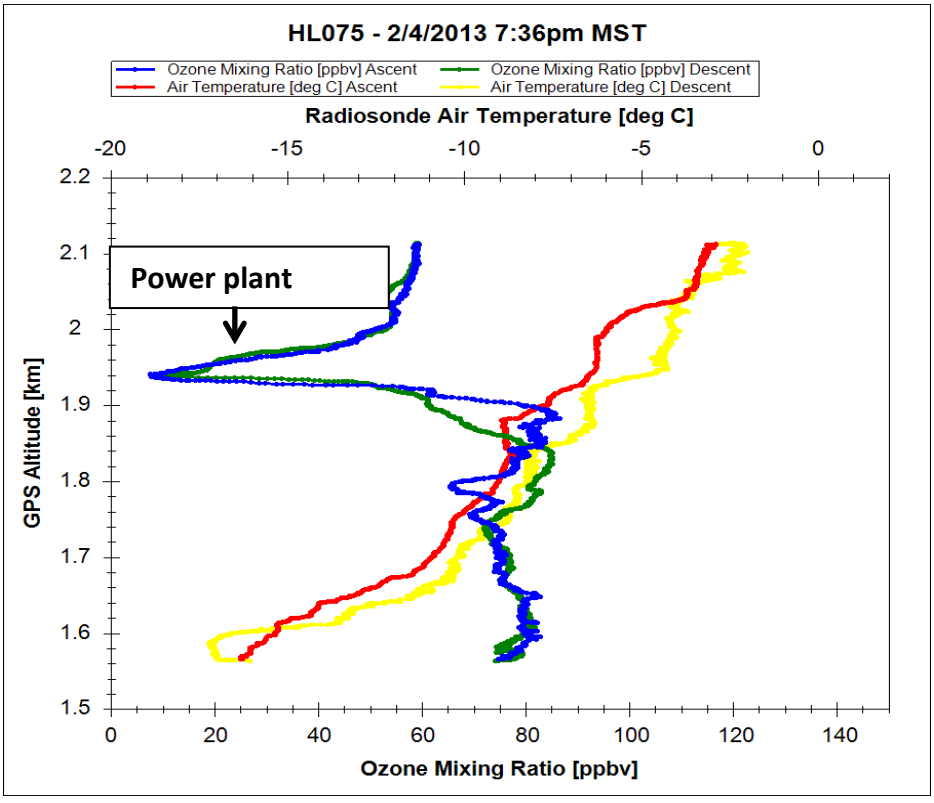

Figure 8-45. Horsepool ozone and temperature profiles on February 4, 2013 showing a well-mixed ozone layer up to 1850 m and the Bonanza plume at 1940 m.

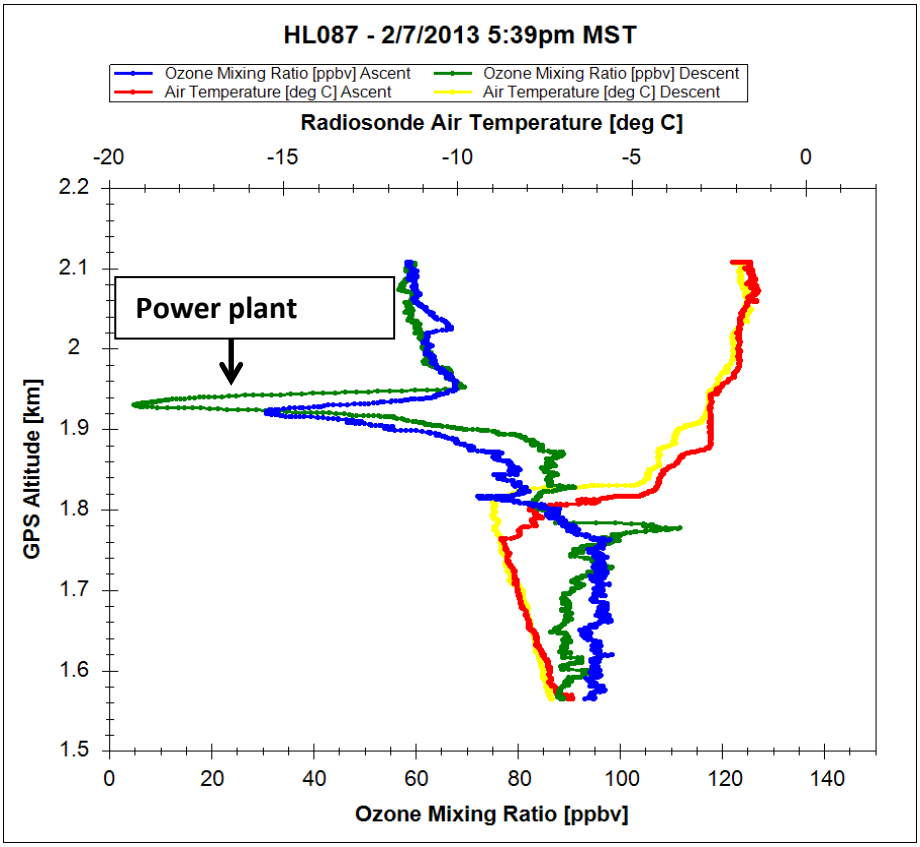

Figure 8-46. Horsepool ozone and temperature profiles on February 7, 2013 showing the surface ozone layer capped at 1780 m and the Bonanza power plant plume centered at 1920 m.

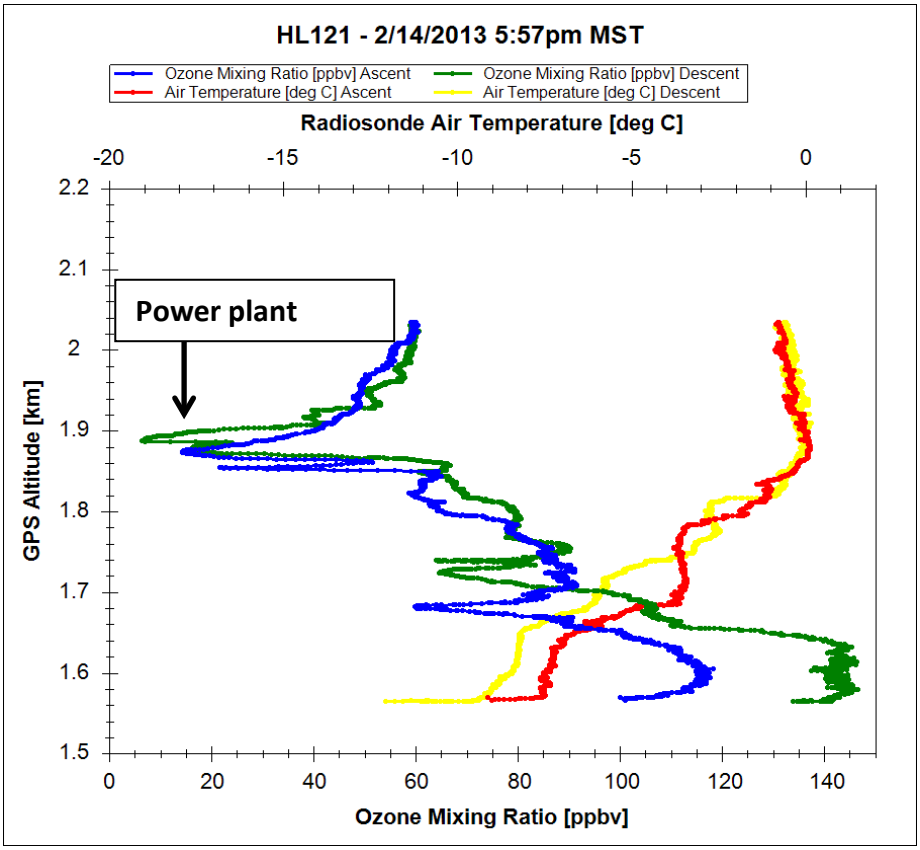

Figure 8-47. Horsepool ozone and temperature profiles on February 14, 2013 showing a strong surface ozone layer capped at 1620 m and the power plant plume centered at 1860 m. This profile complements the data presented in Figure 48-9.

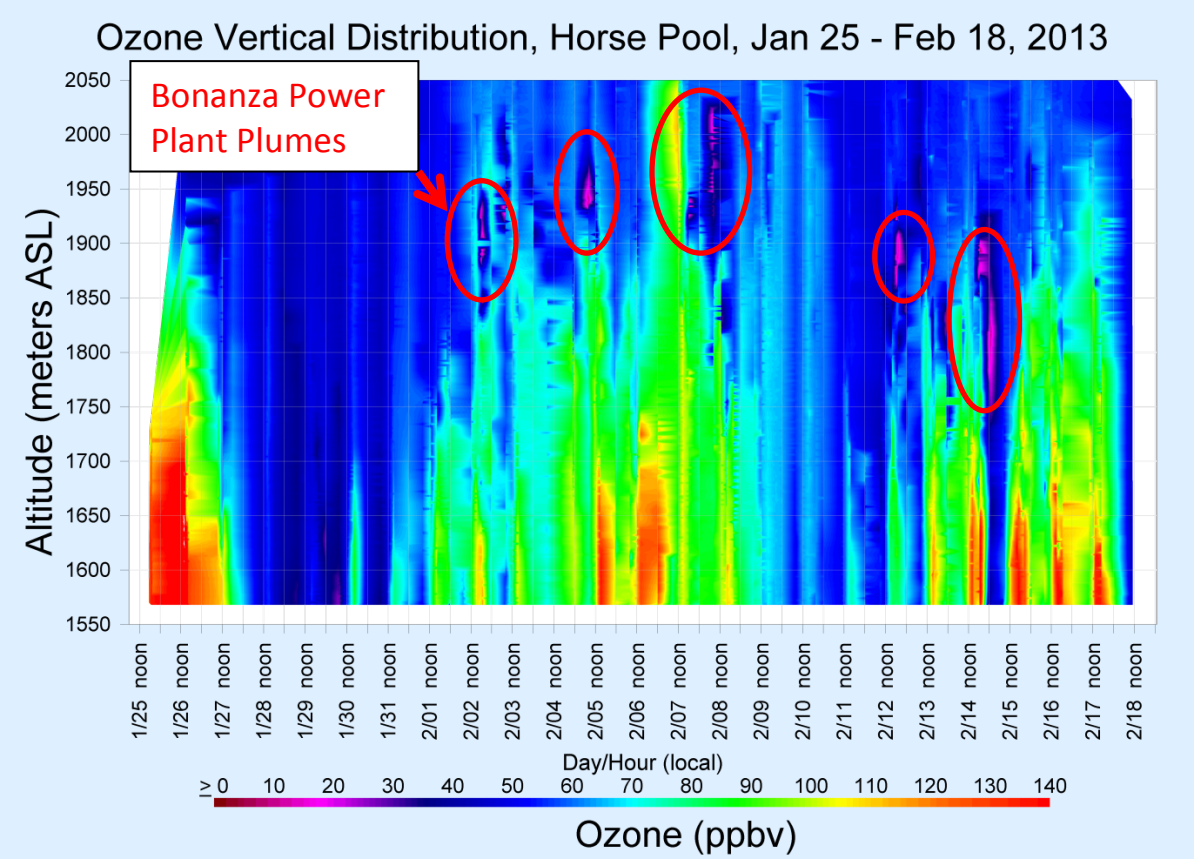

Figure 8-48. Time-height cross section of ozone concentrations measured by tethersondes over Horsepool January 25 - February 18, 2013 with the Bonanza power plant plumes highlighted. The plume on the night of February 14 during the cleanout was probably pushed down to 1800 m by the fresh air descending into the basin.

8.3.3 Tunable Optical Profiler for Aerosol and Ozone (TOPAZ) Lidar Measurements from Horsepool

During UBOS 2013, the NOAA TOPAZ lidar located at Horsepool occasionally observed ozone titration as the NO_x-rich plume from the nearby Bonanza power plant was advected over the Horsepool site. As an example, the data in Figure 8-49 shows a two-hour time-height cross section from near the surface up to 600 m agl (2100 m asl) on the evening of 14 February with the coincident profile of the ozone tethersonde data as presented in Figure 8-47. Both lidar and ozonesonde show the Bonanza plume at ~350 m agl (~1900m asl). Contrary to UBOS 2012, low ozone values were confined to the upper part of the cold-pool layer above the boundary layer. This suggests that power plant NO_x was very likely not a significant part of the precursor mix that led to the high surface ozone values observed in 2013.

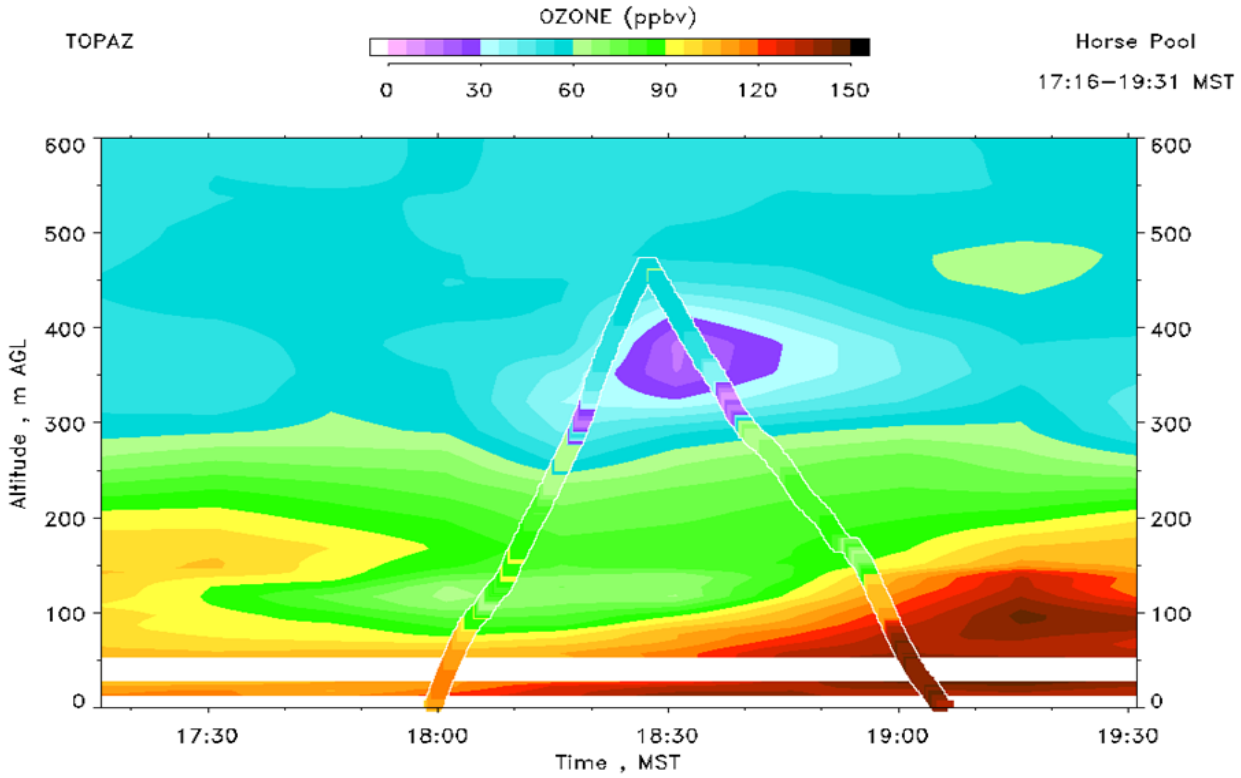

Figure 8-49. TOPAZ time-height cross section of ozone from near the surface to 600 m AGL (2100 m) for 17:16 – 19:31 MST on 14 February 2013 at Horsepool. The colored line shaped like an inverted "V" represents the ozone measurements from the collocated tethersonde data presented in Figure 8-47.

8.3.4 Physical Boundaries to Ozone Production and Precursors in the Uinta Basin

Wintertime ozone production in the Uinta Basin, when there is snow cover on the ground, is confined to a relatively shallow boundary layer capped by a stable temperature inversion. In the winter of 2013 this inversion was level across the basin varying from 1600 to 1700 m. In Figure 8-50, the purple area falls approximately within the 1600 m contour within which ozone was always elevated in the 2013 events and the boundary between the turquoise and green shading approximates the 1700 m contour under which the photochemical ozone production occurred. As such, the precursors for the ozone production reactions have to also be beneath the 1700 m contour and for the most part beneath the 1600 m contour. From this figure it may also be suggested that both Dinosaur and Rangely, Colorado could occasionally be within the Uinta Basin ozone production zone when there are weak or elevated temperature inversions, or when west winds in the basin move precursors and ozone east.

In Figure 8-51 are plotted the oil and gas wells in the basin along with the elevation contours. From this figure it may be observed that many of the western oil wells are above the top of the inversion and thus may not be contributing precursor emissions to ozone production within the basin to as great an extent as wells located well below the inversion. Almost all gas wells (one of the ozone precursor sources) in Uintah County are beneath the 1700 m inversion level.

Surface Elevation Contours in the Uinta Basin, Utah

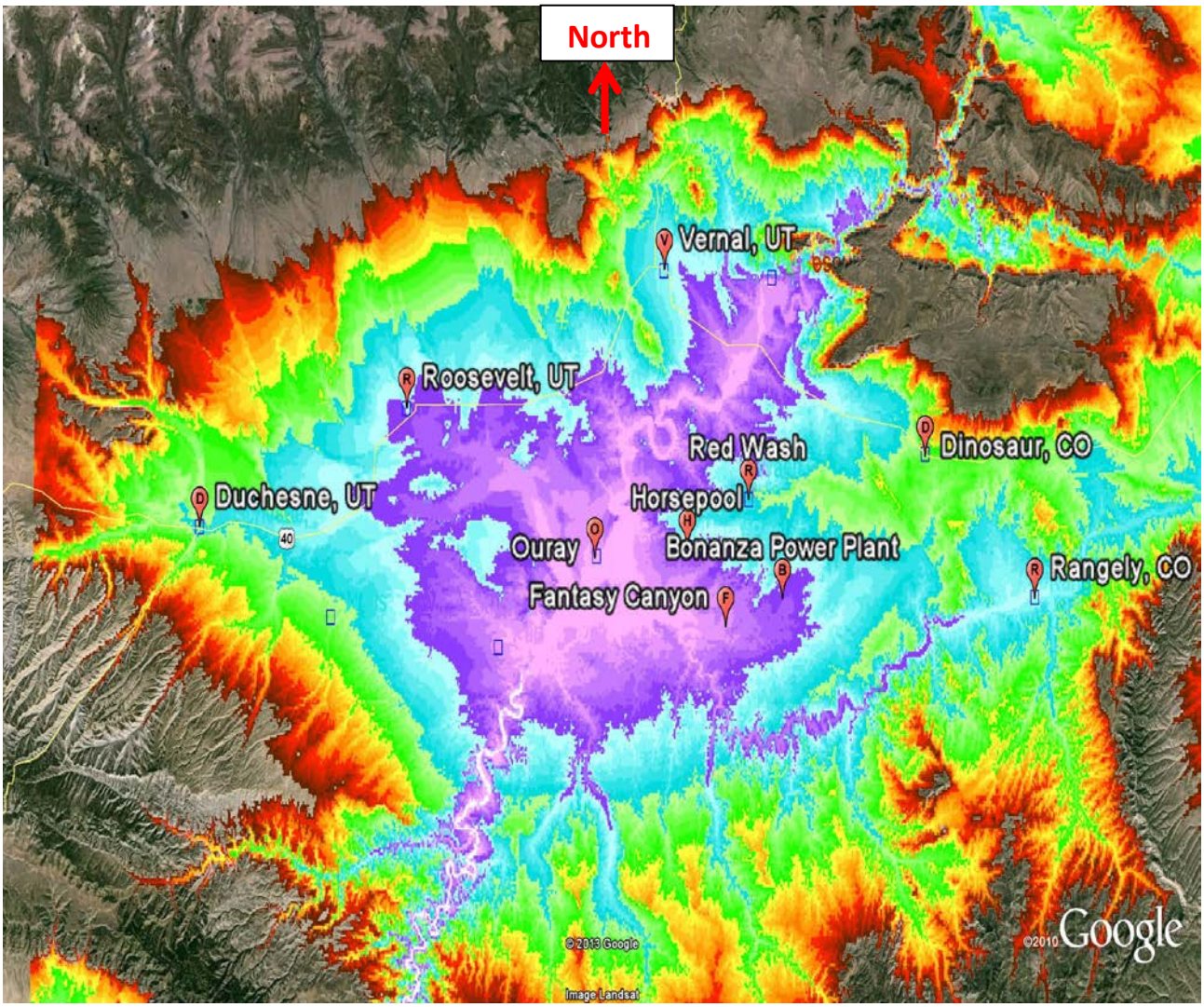

Figure 8-50. Uinta Basin surface elevation contours where the purple hue delineates the lowest elevations in the basin bounded on the upper side by the ~1600 m contour. The boundary between the turquoise and green hues is the ~1700 m contour. Rapid, high concentration photochemical ozone production in the winter of 2013 occurred almost exclusively beneath the level of the 1700 m contour. The most frequent and intense ozone production occurred below 1600 m elevation. Rangely, Colorado is just within this zone as is Duchesne, Utah. The town of Dinosaur, Colorado near the Dinosaur National Monument is just on the edge of the high ozone production zone. Dinosaur could well experience elevated ozone under weak inversions or low altitude westerly winds.

Oil and Gas Wells and Surface Elevation Contours in the Uinta Basin, Utah

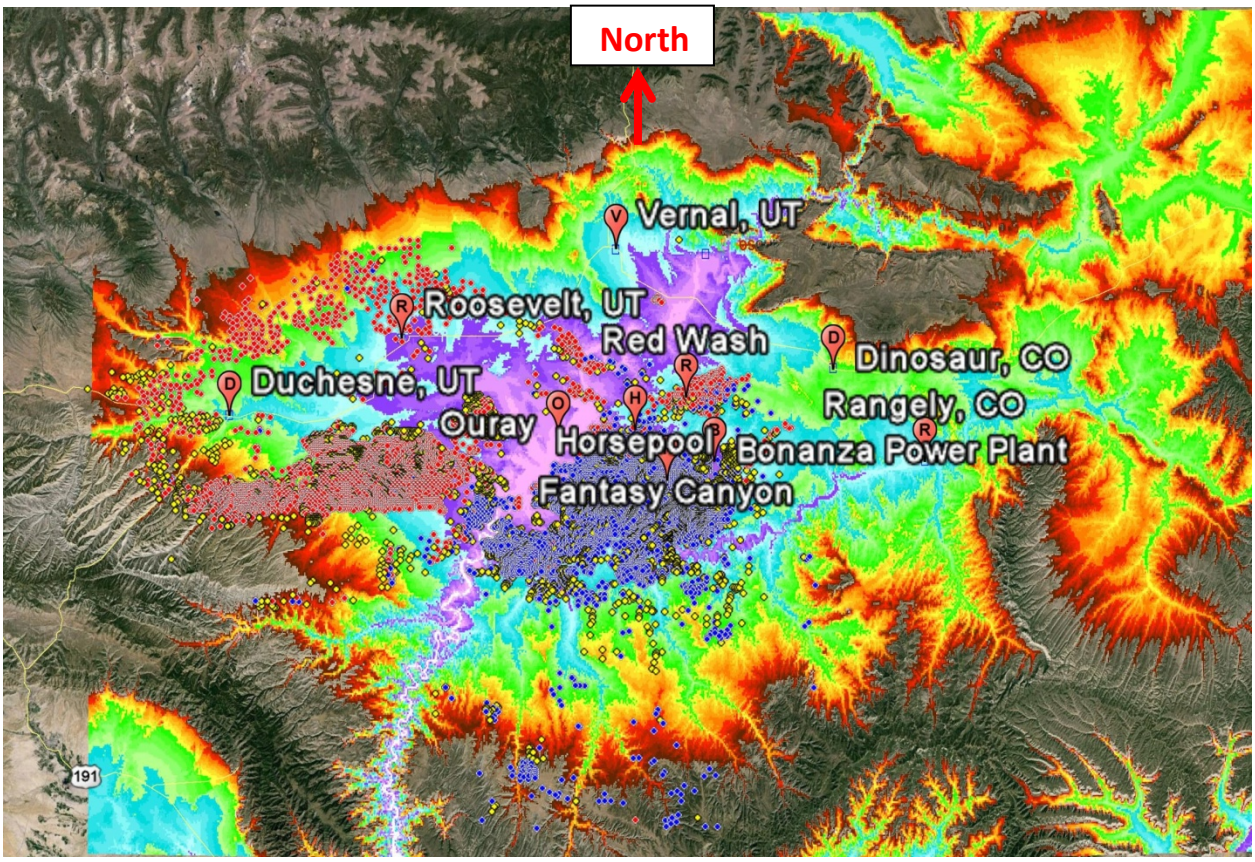

Figure 8-51. Oil and gas wells plotted along with elevation contours. A large number of the western basin oil wells are at elevations above the 1600 -1700 m elevation of the temperature inversions and thus may not be significantly contributing precursor chemicals to the ozone production that occurs lower down in the Uinta Basin. This needs to be checked with mobile van measurements.

8.4 Conclusions

A. The wintertime photochemical ozone production in the Uinta Basin requires snow on the ground, a shallow boundary layer, stagnation and a persistent temperature inversion capping the shallow ozone production layer. The snow helps to keep the surface cold reinforcing the production and maintenance of temperature inversion, reflects daytime solar radiation that enhances photochemical ozone production, and may be involved in snow chemistry as discussed in other sections of this report. The inversion layer traps gaseous effluents from the wells, pipelines, compressor stations and vehicle exhausts in a shallow layer where the rapid photochemical ozone production occurs.

B. During high ozone events, the tethersonde data show that air in the Uinta Basin below 1650-1700m is isolated from the rest of the atmosphere and emissions at the surface are trapped in this shallow layer (see sections 4 and 6, Aircraft and Horsepool balloon measurements respectively). The ozone precursors have to be coming from within the Uinta Basin below the 1700 m contour. There is some horizontal and vertical transport within the basin with some of the ozone mixing up through the inversion layer.

C. Within a few hours of a strong temperature inversion onset with a snow covered ground, ozone production begins during daylight hours and peaks around 2-3 hours after solar noon. This photochemical production can produce up to 60 ppb of ozone through a 250 m layer of the atmosphere within 4 hours. Once an ozone event is in progress, nighttime titration of ozone may only remove 10-20 ppb ozone. Thus, successive days build upon the elevated ozone levels of the previous day. Within 2-3 days of an ozone event, nighttime ozone concentrations can remain above 75 ppb and reach up to 160 ppb during the day.

D. Based on the tethersondes data from Horsepool and Fantasy Canyon, the Bonanza power plant plume was injected above the inversion layer and therefore was not a major source of ozone precursors in the shallow surface inversion layer during high ozone events in the winter of 2013.

E. The battery operated tethersonde system developed for the Uinta Basin ozone studies is an effective instrument for providing numerous continuous profiles of ozone, temperature and humidity semi-automatically from remote sites. A free flying ozonesonde costs about $1200 per launch and produces one profile. The tethersonde can produce more than 100 profiles (2 to 4 per hour) with high vertical resolution for about the same cost as one free flying ozonesonde.

8.5 Outreach and Education in 2012:

The tethered balloon ozonesonde system was set up for 3 different public relation events for the 2012 study. No similar public events were conducted during the 2013 study. In 2012, along with talks and slideshows, the balloons worked very well as a visual aid showing actual scientific measurements of ozone from the balloon tethersondes. Presentations were given during the Winter Ozone Study Kickoff Event at the Bingham Research Center press conference and two local schools: Uintah River High School in Fort Duchesne and Vernal Middle School.

Figure 8-52. Presentation and balloon demonstration at Uintah River High School in Fort Duchesne, Utah.

Figure 8-53. Presentation and balloon demonstration at Vernal Middle School.

8.6 Acknowledgements

A. The NOAA Global Monitoring Division greatly appreciated the permission, access to power, and the excellent physical facilities for operating an ozonesonde system for the 2013 study at the Ouray National Wildlife Refuge Site (Wildlife Refuge Rd., Ouray, UT). Thanks to Dan Schaad (Refuge Manager) and his capable and accommodating staff.
B. We thank the staff at the EDL Bingham Research Center for support during both campaigns and to Questar Resources for access to the Blue Feather Pipe Yard for operating an ozone monitor.
C. Funding for the campaigns came from NOAA, EPA and a consortium of industry resources represented by the Western Energy Alliance.

8.7 References

Deshler, T., et al., Atmospheric comparison of electrochemical cell ozonesondes from different manufacturers, and with different cathode solution strengths: The Balloon Experiment on Standards for Ozonesondes, *J Geophys Res-Atmos*, 113(D4), 2008.

Komhyr, W.D., Electrochemical concentration cells for gas analysis, *Ann. Geophys., 25*, 203-210, 1969.

Komhyr, W.D., R.A. Barnes, G.B. Brothers, J.A. Lathrop, and D.P. Opperman, Electrochemical concentration cell ozonesonde performance evaluation during STOIC 1989, *J. Geophys. Res*., 100, 9231-9244, 1995.

Martin, R., K. Moore, M. Mansfield, S. Hill, K. Harper, and H. Shorthill, Final Report: Uintah Basin Winter Ozone and Air Quality Study, December 2010 – March 2011., *Energy Dynamics Laboratory, Utah State University Research Foundation Report,* Document Ndo appumber EDL/11-039, June 14, 2011.

Morris, Gary A., Walter D. Komhyr, Jun Hirokawa, James Flynn, Barry Lefer, Nicholay Krotkov, Fong Ngan, A balloon sounding technique for measuring SO_2 plumes. *J. Atmos. Oceanic Technol*., 27, 1318–1330. doi: 10.1175/2010JTECHA1436.1, 2010.

Smit, H. G. J., et al., Assessment of the performance of ECC-ozonesondes under quasi-flight conditions in the environmental simulation chamber: Insights from the Juelich Ozone Sonde Intercomparison Experiment (JOSIE), *J Geophys Res-Atmos*, 112(D19), 2007.

Contact:

Bryan Johnson
U.S. Department of Commerce
NOAA/ESRL, 325 Broadway, R/GMD1
Ozone & Water Vapor Group
Boulder, CO 80305-3328
phone: (303) 497-6842
email: bryan.johnson@noaa.gov

2012 DATA FTP site: ftp://ftp.cmdl.noaa.gov/ozwv/ozone/Uintah/DATA_NOAA_Balloon
2013 DATA FTP site: ftp://ftp.cmdl.noaa.gov/ozwv/ozone/Uintah_2013_Tether_OzoneSondes/